

JPRS-UPM-90-004
31 OCTOBER 1990



**FOREIGN
BROADCAST
INFORMATION
SERVICE**

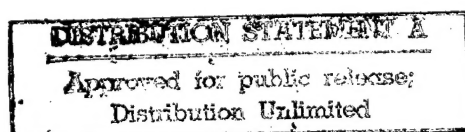
JPRS Report

Science & Technology

USSR: Physics & Mathematics

DTIC QUALITY INSPECTED 3

REPRODUCED BY
U.S. DEPARTMENT OF COMMERCE
NATIONAL TECHNICAL INFORMATION SERVICE
SPRINGFIELD, VA. 22161



19980123 179

Science & Technology

USSR: Physics & Mathematics

JPRS-UPM-90-004

CONTENTS

31 OCTOBER 1990

Acoustics

- Laws of Heat Transfer in Three-Dimensional Viscous Shock Layer of Stream Flowing Past Blunt Bodies at Some Angles of Attack and Glide
[A.I. Borodin, S.V. Peygin; INZHENERNO-FIZICHESKIY ZHURNAL, Vol 58 No 2, Feb 90] 1
- Acoustic Stabilization of Laser Beam Wavefront in Nonhomogeneous Gaseous Medium
[D.O. Lapotko, O.G. Martynenko; INZHENERNO-FIZICHESKIY ZHURNAL, Vol 58 No 2, Feb 90] .. 1
- Relation Between Flammability of Solid Explosives and Their Sensitivity to Impact or Shock-Wave Action
[L.G. Strakovskiy; FIZIKA GORENIYA I VZRYVA, Vol 26 No 1, Jan-Feb 90] 1
- Simple Proofs of Reaction Rate Depending on Deformation Rate of Matter by Detonation Wave
[V.S. Trofimov, G.P. Trofimova; FIZIKA GORENIYA, Vol 26 No 1, Jan-Feb 90] 2

Lasers

- Passive Mode Locking in Optically Pumped $Al_2O_3:Ti^{3+}$ Laser
[M.I. Demchuk, A.A. Demidovich, et al; KVANTOVAYA ELEKTRONIKA, Vol 17 No 2, Feb 90] 3
- Possibility of Raising Efficiency of Free-Electron Laser in Longitudinal Magnetic Field
[V.A. Bazylev, A.V. Tulupov; KVANTOVAYA ELEKTRONIKA, Vol 17 No 2, Feb 90] 3
- Amplification of 172 nm Light in Atmospheric-Pressure Xenon Excited by High-Intensity Proton Beam
[A.A. Kuznetsov, S.S. Sulakshin; KVANTOVAYA ELEKTRONIKA, Vol 17 No 2, Feb 90] 3
- Quantum Fluctuations in Laser With Intracavity Frequency Doubling
[A.I. Zhiliba; OPTIKA ATMOSFERY, Vol 2 No 10, Oct 89] 3
- Copper Vapor as Active Medium for High-Power Oscillator-Amplifier Laser Systems
[N.A. Lyabin, V.V. Zubov, et al; KVANTOVAYA ELEKTRONIKA, Vol 17 No 1, Jan 90] 4
- Characteristics of Excimer Laser With Narrow Emission Line
[K.A. Valiyev, L.V. Velikov, et al; KVANTOVAYA ELEKTRONIKA, Vol 17 No 1, Jan 90] 4
- Intracavity Second-Harmonic Generation by Laser With Optical Delay Line and Mode Locking
[N.S. Balashov, S.K. Isayev, et al; KVANTOVAYA ELEKTRONIKA, Vol 17 No 1, Jan 90] 5

Nuclear Physics

- New Effects in Scattering of Charged Particle by Cosmic String
[Ya.I. Kogan, K.G. Selivanov; ZHURNAL EKSPERIMENTALNOY I TEORETICHESKOY FIZIKI, Vol 97 No 2, Feb 90] 6
- Acceleration of Decay of ^{235m}U -Nucleus Owing to Laser-Stimulated Resonant Internal Conversion
[B.A. Zon, F.F. Karpeshin; ZHURNAL EKSPERIMENTALNOY I TEORETICHESKOY FIZIKI, Vol 97 No 2, Feb 90] 6
- Propagation of Femtosecond Solitons Through Single-Mode Optical Fibers
[A.B. Grudin, V.N. Menshov, et al; ZHURNAL EKSPERIMENTALNOY I TEORETICHESKOY FIZIKI Vol 97 No 2, Feb 90] 6
- Equation of State for Cesium and Speed of Sound in Cesium at Temperatures Up to 2200 K Under Pressures Up to 60 MPa
[V.F. Kozhevnikov; ZHURNAL EKSPERIMENTALNOY I TEORETICHESKOY FIZIKI Vol 97 No 2, Feb 90] 6
- New Mechanism of NN Annihilation Into Three Mesons in Constituent Quark Model
[Yu.S. Kalashnikova, V.P. Yurov; YADERNAYA FIZIKA, Vol 51 No 2, Feb 90] 7
- New Patterns in Hadron Mass Spectrum
[A.B. Kaydalov; YADERNAYA FIZIKA, Vol 51 No 2, Feb 90] 7
- Three-Particle Electron Attachment to O_2 Molecule in CO_2 Plasma
[N.L. Aleksandrov, S.M. Kurkin, et al; KHIMICHESKAYA FIZIKA, Vol 8 No 9, Sep 89] 8
- Ternary Fission of Neutron-Excited Uranium Fissioning Isomers
[V. Ye. Mararenko, Yu. D. Molchanov, et al.; YADERNAYA FIZIKA, Vol 50 No 4, Oct 89] 8

Role of Structural Stability in Changing Microjunction Spectra of Zn Single Crystals [V.N. Nikiforenko, F.F. Lavrentyev; IZVESTIYA VYSSHIKH UCHEBNYKH ZAVEDENIY: FIZIKA, Vol 32 No 12, Dec 89]	8
S-Matrix Formalism for Calculating Probabilities of Atomic Transitions With Polarization Effects [A.V. Glushkov, S.V. Malinovskaya, et al; IZVESTIYA VYSSHIKH UCHEBNYKH ZAVEDENIY: FIZIKA, Vol 32 No 12, Dec 89]	9
Problems in Optimization of Target Use for Neutron Generators [G.I. Primenko, V.I. Strizhak, et al; UKRAINSKIY FIZICHESKIY ZHURNAL, Vol 34 No 12, Dec 89]	9
Frequency-Modulation Spectroscopy With Light in Compressed State [M.V. Danilenko, V.I. Romanenko, et al; UKRAINSKIY FIZICHESKIY ZHURNAL, Vol 34 No 12, Dec 89]	9
Search for Narrow Diproton Resonances [L.S. Vorobyev, V.B. Gavrilov, et al; YADERNAYA FIZIKA, Vol 51 No 1, Jan 90]	9
Masses of Neutrinos in Left-Right Symmetry Models [G.M. Asatryan, A.N. Ioannisyann; YADERNAYA FIZIKA, Vol 51 No 1, Jan 89]	10
Search for Massive Neutrinos in Reactor of Rovno AES [V.I. Kopeykin, L.A. Mikaelyan, et al; PISMA V ZHURNAL EKSPERIMENTALNOY I TEORETICHESKOY FIZIKI, Vol 51 No 2, 25 Jan 90]	10
Phase Conjugation by Four-Wave Interaction in Molten Solution [S.A. Viznyuk, P.P. Pashikin, et al; PISMA V ZHURNAL EKSPERIMENTALNOY I TEORETICHESKOY FIZIKI, Vol 51 No 2, 25 Jan 90]	10
Spin Depolarization of Muons in Condensed Nitrogen [V.G. Grebennik, V.N. Duginov, et al; PISMA V ZHURNAL EKSPERIMENTALNOY I TEORETICHESKOY FIZIKI, Vol 51 No 1, 10 Jan 90]	11
Nuclear-Magnetic Resonance Spectra of ^{205}Tl in $\text{Ti}_2\text{Ba}_2\text{Ca}_n\text{Cu}_{n+1}\text{O}_{6+2n}$ High- T_c Superconductors With $n = 0, 1, 2$. [N.Ye. Alekseyevskiy, G.M. Kuzmicheva, et al; PISMA V ZHURNAL EKSPERIMENTALNOY I TEORETICHESKOY FIZIKI, Vol 51 No 1, 10 Jan 90]	11
Relativistic Polarization Potential of Multi-Electron Atom [A.V. Glushkov; IZVESTIYA VYSSHIKH UCHEBNYKH ZAVEDENIY: FIZIKA, Vol 33 No 1, Jan 90]	12
New Exact Solutions to Schroedinger Equation Based on Finite-Dimensional Matrices [O.B. Zaslavskiy; IZVESTIYA VYSSHIKH UCHEBNYKH ZAVEDENIY: FIZIKA, Vol 33 No 1, Jan 90]	12
Solution of One-Dimensional Problem in Nonlinear Theory of Elasticity With Structured Shock Wave [A.A. Burenin, Yu.A. Rossikhin; PRIKLADNAYA MEKHANIKA, Vol 26 No 1, Jan 90]	12
Constructing Mathematical Model of Adaptive Anti-Flutter System [B.O. Kachanov, S.I. Ovcharenko, et al; PRIKLADNAYA MEKHANIKA, Vol 26 No 1, Jan 90]	12

Optics, Spectroscopy

Present Status and Outlook for Development of Optical Scanning Microscopy [V.G. Dyukov, Yu.A. Kudiyarov; IZVESTIYA AKADEMII NAUK SSSR: SERIYA FIZICHESKAYA, Vol 54 No 2, Feb 90]	14
Recording Femtosecond Pulses of Ultraviolet Light by Two-Photon Luminescence of CsI:Na Crystal [R.G. Deutsch, F. Noack, et al; PISMA V ZHURNAL TEKHNICHESKOY FIZIKI, Vol 16 No 3, Feb 90]	14
Formation of Fractal Structures During Explosion [A.P. Yershov, A.L. Kupershtokh, et al; PISMA V ZHURNAL TEKHNICHESKOY FIZIKI, Vol 16 No 3, Feb 90]	14
Nonlinear Optical Absorption of Light in KS-19 Glass [N.R. Kulish, V.P. Kunets, et al; UKRAINSKIY FIZICHESKIY ZHURNAL, Vol 35 No 2, Feb 90]	15
Microsecond-Pulse Nd-Glass Laser With Monopulse Duration Control [B.V. Anikeev, V.V. Krutyakov; UKRAINSKIY FIZICHESKIY ZHURNAL, Vol 35 No 2, Feb 90]	15
Breakup of Femtosecond Pulses During Amplification in Er^{3+} -Doped Single-Mode Optical Fibers [A.B. Grudin, Ye.M. Dianov, et al; PISMA V ZHURNAL EKSPERIMENTALNOY I TEORETICHESKOY FIZIKI, Vol 51 No 3, Feb 90]	15
Electron-Hole Droplets or Laser Effect in Germanium Crystals? [A.A. Kipen; PISMA V ZHURNAL EKSPERIMENTALNOY I TEORETICHESKOY FIZIKI, Vol 51 No 3, Feb 90]	16

Magnetostriction in $\text{PrBa}_2\text{Cu}_3\text{O}_{7-\delta}$ Single Crystal [A.K. Zvezdin, A.M. Kadomtseva, et al; PISMA V ZHURNAL EKSPERIMENTALNOY I TEORETICHESKOY FIZIKI, Vol 51 No 3, Feb 90]	16
Accounting for Refraction in Optical Tomography [B.F. Apter, B.Ye. Kunber; OPTIKA I SPEKTROSKOPIYA, Vol 67 No 6, Dec 89]	16
He-Ne Laser Emitting Five Lines Simultaneously [Ya.M. Bondarchuk, R.M. Voznyak, et al; OPTIKA I SPEKTROSKOPIYA, Vol 67 No 6, Dec 89]	17
Vacuum-Ultraviolet Characteristics of New Fluoride Matrix [K.M. Devyatkov, O.N. Ivanova, et al; DOKLADY AKADEMII NAUK SSSR, Vol 310 No 1, Jan 90] ...	17
Origin of Residual Surface Resistance of Ceramic High-Temperature Superconductors [N.V. Fomin; PISMA V ZHURNAL TEKHNIЧЕСКОY FIZIKI, Vol 16 No 1, Jan 90]	17
Experimental and Theoretical Study of Forces and Spatial Resolution in Atomic Force Field Microscope [Yu.N. Moiseyev, V.I. Panov; ZHURNAL TEKHNIЧЕСКОY FIZIKI, Vol 60 No 1, Jan 90]	18
Factors Limiting Duration of Pulsed Electron Beam Formed Along Climbing Magnetic Field in High-Current Diode [V.G. Kovalev, O.L. Komarov, et al; ZHURNAL TEKHNIЧЕСКОY FIZIKI, Vol 60 No 1, Jan 90]	18
Limiting Pulse Signal in NbN-Si Structure: Superconductor Film on Substrate [Ye.F. Gatsura, A.B. Kozyrev, et al; ZHURNAL TEKHNIЧЕСКОY FIZIKI, Vol 60 No 1, Jan 90]	19
Increasing Speed of Adaptive Control of Light-Beam Front in Multidither Algorithm, Part 2: Practical Implementation of Algorithms [V.A. Trofimov; OPTIKA ATMOSFER, Vol 3 No 1, Jan 90]	19
Multiline Representation of Integral Radiation Absorption in Molecular Bands [A.G. Ishov, N.V. Krymova; OPTIKA ATMOSFER, Vol 3 No 1, Jan 90]	19

Superconductivity

Effect of Paramagnetic Impurities on Dynamics of Magnetic Fluxes in Superconductors [Yu.I. Gorobets, A.N. Kuchko, et al; UKRAINSKIY FIZICHESKIY ZHURNAL, Vol 35 No 1, Jan 90] ..	20
Phenomenological Theory of Phase Transitions to Nonhomogeneous Noncommensurate Phase With Superconducting Current [A.M. Prokhorov, A.Ya. Braginskiy, et al; DOKLADY AKADEMII NAUK SSSR, Vol 310 No 3, Jan 90]	20
Nonuniqueness of Autowave Modes of Switching Wave Propagation Through Media With Memory [S.L. Sobolev; DOKLADY AKADEMII NAUK SSSR, Vol 310 No 3, 30 Jan 90]	20
Thermal Conductivity of High-Temperature Superconductors in Normal State [A. Jezowski, J. Klamut; FIZIKA NIZKIKH TEMPERATUR, Vol 15 No 10, Oct 89]	21
Superconductivity of Oxide Film Electrolytically Deposited on Surface of $\text{Bi}_{1-x}\text{Sb}_x$ Single Crystal [V.N. Alfeyev, B.A. Aminov, et al; FIZIKA NIZKIKH TEMPERATUR, Vol 15 No 10, Oct 89]	21
Effect of Hydrogen on $\text{YBa}_2\text{Cu}_3\text{O}_y$ Ceramic With $y = 6.91$ and 6.54 [V.V. Sinitsyn, I.O. Bashkin, et al; FIZIKA TVERDOGO TELA, Vol 31 No 12, Dec 89]	22
Transformation of Acoustic Wave at Piezocrystal-Superconductor Boundary [V.I. Alshits, V.N. Lyubimov; FIZIKA TVERDOGO TELA, Vol 31 No 12, Dec 89]	22
Kinetics of Polymer Breakdown at Moderate and Low Temperatures [A.I. Slutsker, T.M. Veliyev, et al; FIZIKA TVERDOGO TELA, Vol 31 No 12, Dec 89]	22
New Phases in Ti-Ca-Ba-Cu-O and Bi-Ca-Sr-Cu-O Systems [N.Ye. Alekseyevskiy; DOKLADY AKADEMII NAUK SSSR, Vol 310 No 2, Jan 90]	23

Probability, Statistics

Stochastic Model of Quantum Mechanics [V.Yu. Podlipchuk; TEORETICHESKAYA I MATEMATICHESKAYA FIZIKA, Vol 82 No 2, Feb 90] ..	24
New Mechanism of Particle Acceleration and Rotation Number Increase [L.D. Pustynnikov; TEORETICHESKAYA I MATEMATICHESKAYA FIZIKA, Vol 82 No 2, Feb 90] ...	24

Differential Equations

Numerical-Asymptotic Method of Multicomponent Averaging of Equations With Contrasting Coefficients [G.P. Panasenkov; ZHURNAL VYCHISLITELNOY MATEMATIKI I MATEMATICHESKOY FIZIKI, Vol 30 No 2, Feb 90]	25
--	----

Localized Solutions to Second-Order Nonlinear Differential Equation [B.V. Gisin; <i>ZHURNAL VYCHISLITELNOY MATEMATIKI I MATEMATICHESKOY FIZIKI</i> , Vol 30 No 2, Feb 90]	25
Stability Criterion for Solitons [A.B. Givental; <i>TEORETICHESKAYA I MATEMATICHESKAYA FIZIKA</i> , Vol 82 No 1, Jan 90]	25
Comment on Quantization of Hydrogen Atom by Continuous Integral Method [S.N. Storchak; <i>TEORETICHESKAYA I MATEMATICHESKAYA FIZIKA</i> , Vol 82 No 1, Jan 90]	26
New Method of Calculating Phase of Radial Wave Function for Scattering by Spherically Symmetric Potential [T.M. Bandman, S.G. Rautian; <i>ZHURNAL EKSPERIMENTALNOY I TEORETICHESKOY FIZIKI</i> , Vol 96 No 5, Nov 89]	26
Coherent Effects in Generation of Ultrashort Light Pulses by Semiconductor Injection Laser [E.M. Belenov, P.P. Vasilyev; <i>ZHURNAL EKSPERIMENTALNOY I TEORETICHESKOY FIZIKI</i> , Vol 96 No 5, Nov 89]	26
Extremal Solutions to Some Systems of Differential-Operator Equations [V.S. Melnik; <i>UKRAINSKIY MATEMATICHESKIY ZHURNAL</i> , Vol 41 No 11, Nov 89]	27
Asymptotic Behavior of Solutions to One Class of Differential-Functional Equations [Ye.Yu. Romanenko; <i>UKRAINSKIY MATEMATICHESKIY ZHURNAL</i> , Vol 41 No 11, Nov 89]	27
Commutating Differential Operators of Rank 3 and Nonlinear Equations [O.I. Mokhov; <i>IZVESTIYA AKADEMII NAUK SSSR: SERIYA MATEMATICHESKAYA</i> , Vol 53 No 6, Nov-Dec 89]	27
Periodic Solutions to Differential Equations of Evolution Perturbed by Random Processes [A.Ya. Dorogovtsev; <i>UKRAINSKIY MATEMATICHESKIY ZHURNAL</i> , Vol 41 No 12, Dec 89]	27
Reducibility of System of Linear Differential Equations With Quasi-Periodic Coefficients [A.M. Samoylenko; <i>UKRAINSKIY MATEMATICHESKIY ZHURNAL</i> , Vol 41 No 12, Dec 89]	28
Criteria for Asymptotic Stability of Systems of Differential Equations With Periodic Coefficients [N.Ye. Barabanov; <i>DIFFERENTIALNYE URAVNENIYA</i> , Vol 25 No 12, Dec 89]	28
Existence of Average Differential Inclusion [O.P. Filatov; <i>DIFFERENTIALNYE URAVNENIYA</i> , Vol 25 No 12, Dec 89]	28

Group Theory, Combinatorics

Ergodic Expansion of Fluxes on Homogeneous Spaces of Finite Volume [A.N. Starkov; <i>MATEMATICHESKIY SBORNIK</i> , Vol 180 No 12, Dec 89]	29
--	----

UDC 533.6.011

Laws of Heat Transfer in Three-Dimensional Viscous Shock Layer of Stream Flowing Past Blunt Bodies at Some Angles of Attack and Glide

907L0120A Minsk INZHENERNO-FIZICHESKIY
ZHURNAL in Russian Vol 58 No 2, Feb 90 pp 200-206

[Article by A.I. Borodin and S.V. Peygin, Scientific Research Institute of Applied Mathematics and Mechanics at Tomsk State University]

[Abstract] Heat transfer in a three-dimensional thin viscous shock layer of a supersonic stream flowing past blunt bodies is analyzed by solving the applicable system of three dimensionless partial differential transfer equations, specifically for a stream flowing past triaxial ellipsoids of various proportions with the angles of attack and glide included as two additional parameters of the problem. The ellipsoidal body is described in a rectangular Cartesian system of coordinates with the origin at the stagnation point. The transfer equations are formulated in a curvilinear system with the origin at the stagnation point, with two axes of coordinates on the body surface (ξ from 0 to 1, η from 0 to 2π) and the third one (ζ) normal to it. The stagnation point is a singular one for that system of equations and the two sets of coordinates on the body surface are degenerate, both features being explicated by a change to appropriate new independent and dependent variables. The boundary conditions for the system of equations are adhesion to an impermeable body surface and generalized Rankin-Hugoniot conditions at the shock wave. Such a boundary-value problem is solved numerically by the method of finite differences in the $O(\Delta\zeta) + O(\Delta\xi) + O(\Delta^2)$ order of approximation and with and with $\Delta(\eta, \xi)$, characterizing departure of the shock wave, calculated by the method of cyclic difference factorization so as to ensure stability. Calculations on a BESM-6 high-speed computer were made for ellipsoids with both transverse semiaxes b and c varied from 0.3 to 3 (longitudinal semiaxis $a = 1$), the angle of attack α varied from 0 to $\pi/2$, the angle of glide varied from 0 to $\pi/4$, and the Reynolds number varied from 100 to 500,000. Figures 4; references 15.

[UDC 535.326

Acoustic Stabilization of Laser Beam Wavefront in Nonhomogeneous Gaseous Medium

907L0120B Minsk INZHENERNO-FIZICHESKIY
ZHURNAL in Russian Vol 58 No 2, Feb 90 pp 235-238

[Article by D.O. Lapotko and O.G. Martynenko, Institute of Heat and Mass Transfer imeni A.V. Lykov, BSSR Academy of Sciences, Minsk]

[Abstract] Use of acoustic flow for stabilization of the laser beam wavefront propagating through a nonisothermal and thus nonhomogeneous gaseous medium is

considered, on account of its low inertia and controllability. An ultrasonic beam generated by a sound source propagates toward an inhomogeneity and, as sound is being absorbed in the surrounding gas, there is generated a secondary acoustic flow in the same direction which sweeps the inhomogeneity away from the path the laser beam and thus prevents distortion of its wavefront. The effectiveness of such a stabilization is measured in terms of space and time, namely size of the region from which an inhomogeneity must be removed and length of time from emission of the ultrasonic beam to restoration of the laser beam wavefront. The process is analyzed, considering that the coefficient of sound absorption in an irradiated inhomogeneity can be much smaller than, much larger than, or approximately equal to the coefficient of sound absorption in a homogeneous medium depending on whether the inhomogeneity is removed by acoustic flow within the surrounding homogeneous region, or by acoustic flow developing within the inhomogeneity, or by acoustic flow both within and around the inhomogeneity. Calculations are made for two fundamentally different conditions, an acoustic Reynolds number smaller than one corresponding to linear propagation of sound waves through a medium with linear absorption characteristics and an acoustic Reynolds number much larger than one corresponding to propagation of intense sound waves through a weakly absorbing medium which distorts them nonlinearly and, as a consequence, absorbs them fast. This method of stabilization was tested experimentally, the light intensity on the axis of a laser beam entering a nonhomogeneous medium being measured from the moment an ultrasonic beam had also entered the medium to the moment the laser beam wavefront had been restored. This time span was found to almost coincide with that taken for development of secondary acoustic flow. Figures 2; references 5.

UDC 662.215.4

Relation Between Flammability of Solid Explosives and Their Sensitivity to Impact or Shock-Wave Action

907L0090A Tomsk FIZIKA GORENIYA I VZRYVA
in Russian Vol 26 No 1, Jan-Feb 90 pp 125-129

[Article by L.G. Strakovskiy, Moscow]

[Abstract] A semiempirical expression is derived which describes the dependence of the critical pressure for triggering a solid explosive on the ignition time, on the duration of the triggering pulse, and on the density of the material. The derivation is based on the results of special experiments with a high igniting thermal flux of 600-2000 W/cm² and known data pertaining to ignition of five secondary explosives substances: hexahydro-trinitro-triazine (cyclonite, RDX), octahydro-trinitro-triazine, tetranitro-methyl aniline, 2,4,6-trinitrotoluene (TNT), and RDX+TNT 40. The critical

triggering pressure is found to be approximately proportional to the ignition temperature and rather weakly dependent on the triggering pulse duration. The thus obtained flammability data are found to correlate closely with known data on the sensitivity of these explosive substances to impact by a drop of a weight. Tables 3; references 22.

UDC 534.222.2

Simple Proofs of Reaction Rate Depending on Deformation Rate of Matter by Detonation Wave

907L0090B Tomsk FIZIKA GORENIYA I VZRYVA
in Russian Vol 26 No 1, Jan-Feb 90 pp 136-142

[Article by V.S. Trofimov and G.P. Trofimova, Chernogolovka]

[Abstract] Decomposition of an explosive substance by a detonation wave is considered, experimental evidence indicating that the reaction rate depends not only on pressure, volume and chemical composition but also rather strongly on the deformation rate. This has been accounted for theoretically by adding the deformation rate as another argument of the reaction rate function, the temperature appearing implicitly in terms of other

independent variables according to the equation of state for a substance with a variable chemical composition. A simple proof is proposed to validate this, on the basis of five premises: 1) all work done by any particle is objectively describable by the product $p dv$, which implies an isotropic stress tensor; 2) the substance can be described by caloric equation of state, its specific internal energy being a function of pressure, volume, and chemical composition which varies; 3) transport processes are disregarded as of negligible significance, which implies an adiabatic motion of each particle; 4) the reaction rate function is infinitely many times differentiable with respect to each argument; 5) an objective quantity characterizing the reaction rate either increases or remains constant as the internal energy of the charge increases, regardless of the volume and the chemical composition but not pressure, an objective characteristic of the reaction rate being introduced and because the selection of variables characterizing the chemical composition is not a unique one (the same composition can be expressed in several different ways). Following a rigorous definition of this objective reaction rate characteristic, the dependence of the reaction rate on the deformation rate is demonstrated on cast 2,4,6 trinitrotoluene by theoretical analysis of experimental data. Figures 2; references 8.

UDC 621.373.826.038.852.2

Passive Mode Locking in Optically Pumped $\text{Al}_2\text{O}_3\text{:Ti}^{3+}$ Laser

907L0114A Moscow KVANTOVAYA ELEKTRONIKA
in Russian Vol 17 No 2, Feb 90 p 133

[Article by M.I. Demchuk, A.A. Demidovich, N.I. Zhavoronkov, V.P. Mikhaylov, A.P. Shkadarevich, A.A. Ishchenko, and A.I. Sopin, Scientific Research Institute of Problems in Applied Physics imeni A.N. Sevcenko, Minsk]

[Abstract] An experiment involving an optically pumped Ti-activated sapphire crystal AO_3^{3+} grown by the Czochralski method has demonstrated the feasibility of passive mode locking in such a laser. The crystal, a rod 7 mm in diameter and 80 mm long, was pumped by a gas-discharge lamp with flash pulses of 5-100 J energy and 5 μs duration above the half-amplitude level, inside an elliptical reflector with a luminophor based ethanol solution of coumarin-30 dye as coolant. The laser cavity was formed by a spherical 100%-reflectance mirror with a 2.5 m radius and an 85%-reflectance plane. Three prisms made of TFN optical glass were used for wavelength selection and dyes with the matching spectral characteristics served as passive saturable filters. Passive mode locking and emission of ultrashort 25 ps pulses were achieved, tunable over both 750-765 nm and 780-790 nm bands with 2780 dye and with 4409 dye respectively. Figures 2; references 4.

UDC 538.561:621.373.826

Possibility of Raising Efficiency of Free-Electron Laser in Longitudinal Magnetic Field

907L0114B Moscow KVANTOVAYA ELEKTRONIKA
in Russian Vol 17 No 2, Feb 90 pp 156-159

[Article by V.A. Bazylev and A.V. Tulupov, Institute of Atomic Energy imeni I.V. Kurchatov, Moscow]

[Abstract] The possibility of further raising the efficiency of a free-electron laser in a longitudinal magnetic field (ubitron) by providing for a single reflection of the electrons at the ponderomotive potential—and thus their single passage through resonance—is examined theoretically on the basis of electron motion in both magnetic and wiggler fields. The efficiency of such a laser has already been raised by a profiling of its parameters so as to ensure capture of electrons on closed trajectories near the retarding stage as well as by optimization of the magnetic field. The interaction of electrons and the combination-frequency wave is shown to depend largely on a parameter which determines the electron bunching and in the absence of wiggler profiling characterizes anisochronism. As this parameter approaches zero, therefore, the efficiency can increase appreciably toward a higher maximum attainable. As this parameter approaches infinity, on the other hand, the efficiency

remains constant but the phase area of the capture region shrinks toward zero. These conclusions have been confirmed by analytical and then numerical solution of a system of two equations describing the evolution of both amplitude and phase of the light wave. Figures 1; references 11.

UDC 539.9:537.82

Amplification of 172 nm Light in Atmospheric-Pressure Xenon Excited by High-Intensity Proton Beam

907L0114C Moscow KVANTOVAYA ELEKTRONIKA
in Russian Vol 17 No 2, Feb 90 pp 205-206

[Article by A.A. Kuznetsov and S.S. Sulakshin, Scientific Research Institute of Nuclear Physics at Tomsk Polytechnic Institute imeni S.M. Kirov]

[Abstract] An experimental study was made concerning stimulated pulsed emission of 172 nm radiation in xenon upon excitation of the latter by a 500 keV and 200 A/cm² proton beam from an accelerator in pulses of 80 ns duration above the half-amplitude level. The proton beam had a 2 cm thick and 30 cm wide cross-section. It could pump a power of up to 100 MW/cm³ into the xenon under a pressure of 1 atm. The xenon cell was located inside an L=30 cm long optical cavity formed by an Al + MgF₂ coating on a quartz substrate with an $R_2 = 0.70$ reflection coefficient for 172 nm light and a LiF₂ crystal with a not higher than 0.05 reflection coefficient. The intensity of light emission I was measured with the high-reflectance mirror open (I_0) and closed (I_c), the amplification coefficient then being calculated according to the relation $\kappa = L^{-1} \log[(\alpha - 1)/R_2]$ with $\alpha = I_c/I_0$. The maximum gain $\kappa = 6 \text{ m}^{-1}$ with an attendant shortening of the pulse duration to approximately one half was attained, with the mirror open, at a xenon pressure of 3 atm and a pumping power density was 50 MW/cm³. Figures 2; references 1

UDC 621.375.9:535

Quantum Fluctuations in Laser With Intracavity Frequency Doubling

907L0029A Tomsk OPTIKA ATMOSFERY in Russian
Vol 2 No 10, Oct 89 pp 1118-1120

[Article by A.I. Zhiliba, Institute of Atmospheric Optics at Siberian Department, USSR Academy of Sciences, Tomsk]

[Abstract] A source of light with a minimal quantum fluctuations of intensity for ultrasensitive laser spectroscopy is considered, namely one consisting of an active lasing medium and a frequency-doubling nonlinear crystal inside a common cavity. The ability of such a device to generate simultaneously compressed fundamental and second-harmonic radiation or, under the

appropriate optimum condition, second-harmonic radiation only is demonstrated theoretically on the basis of a semiclassical description of the process by a system of two differential equations. Two successive integrations by parts solve this system of equations in the zeroth and then first approximation, sufficiently accurate for a second-harmonic generator. A subsequent quantum-electronic description of this device and analysis of its statistical characteristics on the basis of the Fokker-Planck equation, with positive-definite Glauber phase density and with adiabatic elimination of variables, indicates the feasibility of attenuating shot noise in the low-frequency range of the radiation power spectrum and thus in emission of fundamental radiation. The author thanks V.N. Gorbachev for helpful discussion and Ye.P. Gordov for constructive comments. References 7

UDC 621.373.826.038.823

Copper Vapor as Active Medium for High-Power Oscillator-Amplifier Laser Systems

907L0112A Moscow KVANTOVAYA ELEKTRONIKA
in Russian Vol 17 No 1, Jan 90 pp 28-31

[Article by N.A. Lyabin, V.V. Zubov, and A.D. Chursin]

[Abstract] An experimental study of the GL-201 industrial Cu-vapor laser with electric-discharge pumping was made, the active medium occupying a volume of 350 cm³ and the discharge channel 2 cm in diameter being lengthened from 93 cm to 123 cm. A shield consisting of eight 1.5 cm thick and 120 cm copper strips around the Cu-vapor cell lowered the wave impedance. Heating and excitation of the active medium was effected by pulses coming from a TG11-2500/50 thyatron-rectifier with a submodulator through a 1:2 step-up autotransformer and a filter, the latter consisting of a 0.5 nF capacitor and a compressible stack of ferrite rings serving as a nonlinear variable choke. The active medium was placed inside an optical cavity between a spherical mirror and a plane one, with neon as buffer gas. Its optimum temperature for the maximum laser emission power of 31 W was reached under a neon pressure of 120 mm Hg with 4.3 kW pumping power and 80 ferrite rings, the emission power being only 23 kW with only 3.9 kW pumping power under a neon pressure of 600 mm Hg. For maximum reliability was selected a neon pressure of 180 mm Hg, which lowered the necessary pumping power and the attendant thyatron losses at an only 10% sacrifice of laser output power. Optimum excitation of the active medium was attained with a 160 pF noninductive peaking capacitor bank. Increasing the number of ferrite rings further increased the laser output power, saturation beginning with 180 rings and reaching the 37.5 W level with 230 rings, but the necessary pumping power drawn from the thyatron increased correspondingly to 5 kW. Maximum luminous laser efficiency was attained with 150 rings, 1.1% when referred to power drawn by the discharge circuit and 0.8% when referred to

power delivered by the thyatron-rectifier. Laser operation at the 35 W nominal level with 4.3 kW pumping power required a thyatron plate voltage of 23 kV and discharge current pulses of 0.4 kA amplitude and 140 ns duration. The system was tested in the plain oscillator mode with a cavity formed either by a spherical mirror and a plane one or by two plane mirrors minimizing the beam divergence, also in the superluminance mode with one superluminance beam formed by the entire geometrical entrance aperture of the discharge channel alone and one formed by both the spherical high-reflectance mirror and the exit aperture of the discharge channel. The system was tested in the amplifier mode with a standard GL-201 laser as master oscillator using one convex spherical mirror, an amplifier output power of 51.3 W being attainable in this scheme under optimum conditions. Figures 6; references 6

UDC 621.373.826.038.823

Characteristics of Excimer Laser With Narrow Emission Line

907L0112B Moscow KVANTOVAYA ELEKTRONIKA
in Russian Vol 17 No 1, Jan 90 pp 43-45

[Article by K.A. Valiyev, L.V. Velikov, G.S. Volkov, and D.Yu. Zaroslov, Institute of General Physics, USSR Academy of Sciences, Moscow]

[Abstract] Narrowing the emission line of excimer lasers for ultraviolet photolithography with use of monochromatic objectives is considered as an alternative to costly manufacture of polychromatic precision objectives or wide-aperture wide-field mirrors free of chromatic aberration. Narrowing of the emission line can be and has been experimentally achieved by insertion of a diaphragm and a dispersive element between the laser cell and the plane high-reflectance mirror and of another diaphragm between the laser cell and the plane exit mirror. The dispersive element could be a prism, a diffraction grating, an etalon, or a combination of any of these devices. Considering that the width of the emission line depends on the divergence of the laser beam, the distance L between the two mirrors (length of cavity) and the diameter d of both diaphragms should be matched so as to make the Fresnel number $F = d^2/4\lambda L = 1$ (λ - wavelength of emitted radiation). Experiments were performed with an ELI-71 commercial 308 nm XeCl-laser and with a diffraction grating as dispersive element. The latter was either a reflective one with 2400 lines/mm in an autocollimating position at a 22° angle for reflection in the first order, preceded by a beam-widening tetraprism telescope, or a diffraction grating with 2400 lines/mm in a position for grazing incidence at a 5-10° angle and for the high-reflectance to be located within the -1st order of the diffraction pattern. Coherence measurements and calculations have yielded the dependence of coherence coefficients C_x along the discharge electrodes and C_y across the discharge electrodes on the diaphragm diameter and thus on the beam divergence

without and with a dispersive element. Without a dispersive element, both coefficients were found to increase with decreasing diaphragm diameter: C_x from near 0 and C_y from approximately 0.1 with a 10 mm diaphragm diameter to approximately 0.5 both with a 2 mm diaphragm diameter. With an autocollimating diffraction grating, only the transverse coherence was found to be significant, $C_y = 0.4$, and with grazing incidence this coefficient was found to depend on the incidence angle as well as on the diaphragm diameter. Use of 2 mm diaphragms and the autocollimating diffraction grating with a tetraprism telescope narrowed the emission line of the XeCl- laser to 5 nm, the laser emitting this narrow-band 308 nm radiation in pulses of up to 2 mJ energy. Figures 7; references 8.

UDC 621.373.826

Intracavity Second-Harmonic Generation by Laser With Optical Delay Line and Mode Locking

907L0112C Moscow KVANTOVAYA ELEKTRONIKA
in Russian Vol 17 No 1, Jan 90 pp 64-66

[Article by N.S. Balashov, S.K. Isayev, L.S. Korniyenko, N.V. Kwartsov, L.N. Magdich, V.Yu. Mikhaylov, S.R. Rustamov, and V.V. Firsov, Scientific Research Institute of Nuclear Physics at Moscow State University imeni M.V. Lomonosov]

[Abstract] An experiment has demonstrated the feasibility of raising the peak emission power of a garnet

lasers with mode locking and also raising the efficiency of its intracavity second-harmonic generation by adding an optical delay line and thus lengthening the cavity. The originally "short" cavity was lengthened by tilting the plane mirror, then adding two more plane mirrors and two spherical mirrors. The distances between mirrors and the curvatures of the spherical ones were matched so as to ensure that a Gaussian laser beam formed in the plane of the first plane mirror returned after all reflections with the same radius and wavefront. The two spherical mirrors formed an afocal system, the first one. Inside it was placed another afocal system, the second one, consisting of two confocal lenses. In the experiment a YAG:Nd laser with a garnet 6 mm in diameter and 100 mm long was pumped with a 3.5 kW gas-discharge lamp and a 2 cm long LiIO_3 nonlinear crystal located within the neck of the caustic surface inside the cavity served as frequency doubler. The plane mirror behind this crystal had either a transmission coefficient $T = 0.125$ for extraction of maximum fundamental-frequency radiation or a reflection coefficient $R = 0.995$ for extraction of maximum second-harmonic radiation. All other mirrors had a reflection coefficient $R = 0.995$ for the fundamental 1.06 μm wavelength. The effect of lengthening the cavity on emission of 1.06 μm radiation was to lower the average power but to raise the peak power while lengthening the duration of ultrashort (500 ps) pulses and increasing their repetition rate. The effect on emission of 0.53 μm radiation with mode locking was to raise both the average power and the peak power. Figures 2; tables 1; references 6

New Effects in Scattering of Charged Particle by Cosmic String

907L0107A Moscow ZHURNAL
EKSPERIMENTALNOY I TEORETICHESKOY
FIZIKI in Russian Vol 97 No 2, Feb 90 pp 387-400

[Article by Ya.I. Kogan and K.G. Selivanov, Institute of Experimental and Theoretical Physics]

[Abstract] Interaction of charged particles and a cosmic local (gauge) string is analyzed for scattering effects which so far have been overlooked, one such effect being the quantum analog of Lorentz scattering in the "magnetic" field of a cosmic string and noteworthy being that such strings are essentially analogous to Abrikosov filaments in type-II superconductors. First is considered scattering of slow particles. The amplitude of their scattering in the field of the string is determined from the Dirac equation for a system with minimum coupling, its solutions being classified according to eigenvalues of the angular momentum operator and the latter containing the Pauli matrix. Next is considered scattering of fast particles. The amplitude of their scattering is calculated not in the Born approximation, which in this case becomes irrelevant, but in the eikonal approximation. Application of Huygens' principle yields the wave function for the $x \ll k/m^2$ range, the wave function for the $1/m \ll k/m^2$ range having been found from the solution to the eikonal equation and the Bohm-Aharonov long-range potential having been removed from the region of positive x by a preliminary gauge transformation. Other interesting physical effects are fast scattering of an incident charged-particle beam and separation of the charges by a string oscillating in a plasma or ionized gas. Figures 2; references 17.

Acceleration of Decay of ^{235}mU -Nucleus Owing to Laser-Stimulated Resonant Internal Conversion

907L0107B Moscow ZHURNAL
EKSPERIMENTALNOY I TEORETICHESKOY
FIZIKI in Russian Vol 97 No 2, Feb 90 pp 401-408

[Article by B.A. Zon and F.F. Karpeshin, Voronezh State University imeni Lenin's Komsomol]

[Abstract] The effect of intense electromagnetic radiation and resulting internal conversion on decay of a ^{235}mU -nucleus is analyzed theoretically, this nucleus providing a unique example of a metastable state with only 76 eV energy comparable with the bonding energy of electrons in the outer shells and with half-life of only 26 min. Internal conversion involves transition of an electron to a discrete level and its probability depends on the frequency mismatch between electronic and nuclear transitions, which makes it not only a discrete process but also a resonant one. Two coefficients characterizing such a conversion, namely the ratio of conversion probability to probability of radiative nuclear transition probability and the ratio of discrete conversion probability to photon emission probability are calculated with the aid of the Feynman diagram describing resonant

internal conversion. Next is considered resonant conversion in a laser radiation field, using an appropriate modification of the Feynman diagram, the frequency of laser radiation being selected so as to compensate the mismatch between electronic and nuclear transitions. Estimates based on these calculations indicate that it is in principle possible to control the speed of both the decay and the excitation of this nucleus during respective electronic transitions, the magnitude of the acceleration depending linearly on the intensity of the laser radiation up to the critical one of approximately 10^8 MW/cm^2 and reaching several orders of magnitude. The authors thank D.P. Grechukhin and Yu.N. Demkov for the helpful discussion, also I.M. Band, N.B. Delone, D.F. Zaretskiy, V.A. Krutov, M.A. Listengarten, and M.B. Trzhaskovskiy for interest and individual comments. Figures 2; references 20

Propagation of Femtosecond Solitons Through Single-Mode Optical Fibers

907L0107C Moscow ZHURNAL
EKSPERIMENTALNOY I TEORETICHESKOY
FIZIKI in Russian Vol 97 No 2, Feb 90 pp 449-454

[Article by A.B. Grudinin, V.N. Menshov, and T.N. Fursa, Institute of General Physics, USSR Academy of Sciences]

[Abstract] The nonlinear Schroedinger equation is modified for an adequate description of femtosecond pulse dynamics and soliton evolution in an optical fiber. Two terms are accordingly added on the left-hand side, a third-order term $(1/6)\beta_0''' \delta^3 \Phi / \delta t^3$ which accounts for wave distortion due to dispersion and a first-order term $(2i\beta_0 / \omega_0 n_0) (\delta \Phi^2 \Phi) / \delta t$ which accounts for sluggish nonlinearity. The solution to this new equation is sought in the form of a traveling wave, such a wave possibly being asymmetric and degenerating into a shock wave. The equation is first reduced to a third-order ordinary differential one for the wave amplitude and this equation is then shown to be simplifiable when the coefficients in its five terms (the coefficient of the third-order and thus highest derivative being 1) are interrelated in a certain way. The conditions for self-localization of the time envelope in the form of a "bright" soliton or a "dark" one are then established, the necessary condition for formation of femtosecond soliton-like pulses being that the third derivative β''' be positive. References 20.

Equation of State for Cesium and Speed of Sound in Cesium at Temperatures Up to 2200 K Under Pressures Up to 60 MPa

907L0107D Moscow ZHURNAL
EKSPERIMENTALNOY I TEORETICHESKOY
FIZIKI in Russian Vol 97 No 2, Feb 90 pp 541-558

[Article by V.F. Kozhevnikov, Moscow Institute of Aviation imeni Sergo Ordzonikidze]

[Abstract] The equation of state for cesium covering the 400-2200 K temperature range and the 0-60 MPa pressure range is constructed on the basis of existing and new

experimental data, cesium being eminently suitable as reference standard for validation of theoretical liquid-metal models. In this study the density of liquid cesium and cesium vapor was measured in a bizonal (hot-cold) dilatometer with a molybdenum or tungsten capillary passing through a molybdenum cell inside a molybdenum or tungsten container in the hot compartment, the radioactive method and the electrical resistance method having been used by other researchers. The speed of sound was measured in a molybdenum tube with a molybdenum limiter ring by the pulse phase method, facilitating a highly accurate determination of the propagation time with an error not larger than about 1 ns when specimens not longer than about 1 mm can be used under extreme conditions. These measurements were made with 10 MHz signals along steady-state isobars, the readings having been necessarily checked for reproducibility under rising and dropping temperature. These data supplemented with already known thermodynamical characteristics, which include not only isobaric and isothermal specific heats but also isobaric thermal expansivity as well as isothermal and adiabatic compressibility, have yielded the critical range for cesium on the liquid-gas coexistence curve and a phase diagram with a mean diameter which curves already at a temperature not yet near the critical one. The law of corresponding states has been determined for cesium on this basis. The results define the critical point more precisely than have earlier results, within an anomalously critical range. The isochoric specific heat of liquid cesium was only calculated, direct measurements not being technically feasible, and found to decrease monotonically from about 3R in the vicinity of the melting point to about 2R in the vicinity of the critical point, without subsequently dipping to a minimum at least before 1700 K. The author thanks N.B. Vargaftik, D.I. Arnold, S.P. Naurzakov, E.B. Gelman, and Ye.V. Grodzinskiy for support and assistance, also V.G. Baks for valuable comments. Figures 8; tables 2; references 47

New Mechanism of NN Annihilation Into Three Mesons in Constituent Quark Model

907L0085A Moscow YADERNAYA FIZIKA in Russian
Vol 51 No 2, Feb 90 pp 479-484

[Article by Yu.S. Kalashnikova and V.P. Yurov, Institute of Theoretical and Experimental Physics at State-Supervised Institute of Atomic Energy]

[Abstract] The method of a quark optical potential according to the nonrelativistic constituent quark model which explicitly includes multi-quark states is used for description of S-wave NN-scattering by central pp-interaction, on the premise of an attendant restructurization into three mesons. Analysis of this process is based on the Hamiltonian $H = H_0 + V + V_{hr}$ (V_{hr} denoting

Fermi-Breit chromomagnetic interaction) of that potential model and involves introduction of a new interaction V_c , a fully blocking one with a discrete spectrum ($H_0 + V_{cu} = E_\mu \Psi_\mu$ only, followed by explicit introduction of corresponding blocked states. The wave function Ψ for the 3q3q system is formulated accordingly, whereupon projection of the Schroedinger equation $H\Psi = E\Psi$ onto both the nucleon-antinucleon and meson projectors and onto Ψ_μ yields a system of coupled equations for χ_{NN} and χ_{3M} . The latter contains an operator T representing kinetic energy in the hadron channel and two nonlocal energy-dependent kernels K, U which are interaction operators representing two different restructurization mechanisms. Inasmuch as the K-operator is already known, of further concern are only the U-kernel and the pure effect of blocked states. Calculations and estimates based on the harmonic confinement model and the $SU(4)_H$ -symmetric limit, even though the latter does not quite match inclusion of hyperfine splitting in the NN-channel and in 3q3q states, indicate that the $NN \rightarrow 3M$ process is a consequence of not only pure restructurization but also restructurization through multi-quark states and meson-meson exchanges with a long-range potential. Determining the significance of the quark optical potential requires introduction of the physical meson masses. The authors thank B.O. Krebikov, A.Ye. Kudryavtsev, and I.M. Narodetskiy for many enlightening discussions. Figures 2; tables 1; references 13

New Patterns in Hadron Mass Spectrum

907L0085B Moscow YADERNAYA FIZIKA in Russian
Vol 51 No 2, Feb 90 pp 499-503

[Article by A.B. Kaydalov, Institute of Theoretical and Experimental Physics at State-Supervised Institute of Atomic Energy]

[Abstract] The structure of boson and baryon Regge trajectories is analyzed with the aid of available data on the mass of hadrons corresponding to certain quantum numbers. First are considered boson trajectories for systems which consist of light (u,d)-quarks: trajectories of states with isospins $I = 0$ or 1 and $\sigma P = +1$ or -1 (σ -signature, P -parity), with strangeness $S = 0$ or 1 . These trajectories are found to be nearly linear and also parallel, their slope being $\alpha' = 0.9 \text{ GeV}^{-2}$, except possibly the π -trajectory with either a different slope or curvilinear form. In the range of mass masses M larger than 1 GeV , moreover, trajectories of the pseudoscalar and axial group $\sigma P = -1$ are close to one another and a unity away from those of the $\sigma P = +1$ group, which in the quark model signifies a weak spin-orbital quark-antiquark interaction. The daughter trajectories with the same quantum numbers are theoretically parallel to the main ones, shifted by an integer from the latter, but not much experimental evidence about such states is available. Next are considered baryon trajectories, resonances being found on their daughter trajectories and degenerate states with a given spin but different parity existing even though parity doubling of states is not natural according to known quark models. A comparison of the

boson and baryon mass spectra indicates an approximate supersymmetry above 1 GeV and that the supersymmetric string model accurately describes the dynamics of hadron systems with large spins. Figures 4; references 8

UDC 539.196.6

Three-Particle Electron Attachment to O₂ Molecule in CO₂ Plasma

907L0078A Moscow *KHIMICHESKAYA FIZIKA* in Russian Vol 8 No 9, Sep 89 pp 1219-1224

[Article by N.L. Aleksandrov, S.M. Kurkin, and V.M. Shashkov, Moscow Institute of Engineering Physics]

[Abstract] The three-particle process $e + O_2 + CO_2 \rightarrow O_2^- + CO_2$ is analyzed on the basis of experimental data and a theoretical model, namely the Bloch-Bradbury model of its mechanism. Measurements were made not only at room temperature (293 K) but also at 373 K, the CO₂ pressure being first 100 torr and then 400 torr at each temperature. Discharges in a 20 dm³ large mono-pulse chamber was sustained by a high-energy electron beam with a 125 keV initial electron energy, in a pulses of approximately 100 μ s duration. The current density was varied over the 0.1-3 mA/cm² range. The beam was injected through a window, an aluminum foil. Discharge was maintained over 20 mm gap between a flat metal cathode and an wire-mesh anode. The experimental data confirm the results of calculations and thus indicate that attachment of an electron to O₂ and CO₂ van der Waals molecules provides a principal channel, the O₂⁻ ion then becoming stabilized as a result of V-T and V-V exchanges. The authors thank A.M. Konchakov for calculating the energy distribution of electrons in the CO₂ plasma and L.V. Shachkin for helpful discussions Figures 4; references 12

Ternary Fission of Neutron-Excited Uranium Fissioning Isomers

907L0017A *YADERNAYA FIZIKA* in Russian Vol 50 No 4, Oct 89, pp 928-935

[Article by V. Ye. Mararenko, Yu. D. Molchanov, G. A. Otroshchenko, G. B. Yan'kov]

[Abstract] This study describes an experiment producing ternary fission of uranium fissioning isomers in the reactions $^{236, 238}U(n, n')$ at a mean neutron energy of 4.5 MeV. The results reported from this study cover the two known fissioning isomers of uranium. The measurements were carried out on the electrostatic accelerator of the Kurchatov Institute of Atomic Energy. The pulsed fast neutron flux was produced in a D(d, n)³He reaction by deuterium ion bunches with a pulse repetition frequency of 2 MHz. The spontaneously fissioning isomers of uranium were identified in this study by measuring the half-decay period and the relative probability of nuclear fission through the isomer state. The reported values for the relative probability of nuclear fission

through the SFI state for the mean neutron energy cited above are (1.30 plus/minus 0.01) times 10⁻⁴ for ²³⁶U and (1.48 plus/minus .02) times 10⁻⁴ for ²⁸⁸U. The study establishes that the relative probability of ternary fission of the spontaneously fissioning isomers of uranium grows significantly compared to the case of ternary fission of the nuclei in nonisomeric states. The analysis attributes this to the peculiar nucleon configuration of the isomer states.

UDC 539.292

Role of Structural Stability in Changing Microjunction Spectra of Zn Single Crystals

907L0091A Tomsk *IZVESTIYA VYSSHIKH UCHEBNYKH ZAVEDENIY: FIZIKA* in Russian Vol 32 No 12, Dec 89 pp 65-68

[Article by V.N. Nikiforenko and F.F. Lavrentyev, Institute of Low-Temperature Engineering Physics, USSR Academy of Sciences]

[Abstract] The problem of producing Zn single crystals for microjunction spectroscopy which will be structurally stable under heavy mechanical load in a strong electric field is analyzed, a high-intensity electron flux being known to drive dislocations into a region where the current density is low and deformation by alternating torsion in the [0001] direction being known to establish low-angle twist boundaries which do not collapse when stable so that the microjunction spectra should be reproducible. Combined action of a mechanical load and an electric field on a Zn single crystal in a structurally stable or metastable state is considered accordingly, an experiment having been performed with such a crystal under alternating torsion in the (0001) slip system while carrying a current of 10⁹-10¹⁰ A/cm² density at a temperature of 1.5 K. Reproducible as well as nonreproducible microjunction spectra were recorded, the former indicating a quasi-elastic strain underneath the torsion load and stability of hexagonal dislocation grids determining the distribution of internal stresses. Changes in the structural state of a microjunction regions being indicated by a blurring as well as a decrease of maxima in the electron-phonon interaction spectra and an attendant increase of the background noise level, the latter was found to depend on the microjunction resistance according to the inverse half-power law and on the current density in a negative linear relation. The maximum spectral intensity, meanwhile, was found to fluctuate about a constant level as the microjunction diameter increased. The data also reveal an inverse half-power law dependence of the torsional strength on the product of mean free path for electrons and effective transport cross-section for scattering of electrons. The mean stress necessary for destabilizing a twist boundary is thus determined and found to be proportional to the disorientation angle. The authors thank I.K. Yanson for discussing the results. Figures 2; references 5

UDC 539.184

S-Matrix Formalism for Calculating Probabilities of Atomic Transitions With Polarization Effects

907L0092B Tomsk IZVESTIYA VYSSHIKH
UCHEBNIKH ZAVEDENIY: FIZIKA in Russian
Vol 32 No 12, Dec 89 pp 73-77

[Article by A.V. Glushkov, S.V. Malinovskaya, and V.V. Filatov, Odessa Institute of Technology imeni M.V. Lomonosov]

[Abstract] A simple semiempirical method is developed for calculating the probabilities of radiative atomic transitions on the basis of the S-matrix with polarization of the atom shell and other significant correlation effects taken in account, this being particularly important for accurate calculations pertaining to subjacent configurations and verifiable by precision measurements. Radiative decay of excited states is considered in an atom with only one electron outside the shell. Following the classical replacement of the dipole matrix element $\alpha |r| n$ of a $\alpha \rightarrow n$ transition with the $q |r - \alpha_d r / r_d / r^3|$ polarization of the atom shell by outside particles is formulated from the standpoint of quantum electronics. Calculations based on the relativistic the second-order perturbation theory and the Low scattering theory yield, with the aid of the Gell-Mann relation for adiabatic scattering, the imaginary part of the electron energy of an atom. Calculations have been made by this method for $\alpha \rightarrow n$ transitions in ions of the isoelectronic Na-I series with $Z = 16-40$ (S, Ti, Se, Zr) and in ions of the isoelectronic Al-I series with $Z = 21-40$ (Sc, Co, As, Y). The results agree closely with those obtained by the theoretically rigorous but more tedious method of successive approximations. Tables 2; references 19

UDC 539.1/08

Problems in Optimization of Target Use for Neutron Generators

907L0070A Kiev UKRAINSKIY FIZICHESKIY
ZHURNAL in Russian Vol 34, No 12, Dec 89
pp 1767-1773

[Article by G.I. Primenko, V.I. Strizhak, N.A. Belyusenko, D.L. Broder, and V.M. Neplyuyev, Kiev University imeni T.G. Shevchenko and Institute of Power Engineering imeni G.M. Krzhizhanovskiy, Moscow]

[Abstract] Use of tritium targets in metal carriers for low-voltage 14 MeV neutron generators is comprehensively reviewed, of concern being causes of low neutron yield and neutron flux instability. As the four major causes are identified depletion of active tritium and of deuterium packing by diffusion, thermal decomposition of metal hydrides, cathodic sputtering by incident heavy ions, and formation of metal oxides. The seven known methods of ensuring higher yield and flux stability are: barrier confinement of hydrogen isotopes, splitting the mixed ion beam into homogeneous tritium ion and

deuterium ion beams, using a high-energy deuteron beam, use of gaseous targets not requiring passive tritium carriers and thus minimizing specific energy loss suffered by ions, additional acceleration of the neutron flux, intensification of the target activity combined with intensification of its cooling, trickle feeding the target with tritium through a capillary (Pd), and boosting the energy of the mixed T^+-D^+ ion beam. The review includes data covering 12 neutron generators: NG-12 (USSR), IPSAS (Czechoslovakia), KLTE (Hungary), LOTUS (Switzerland), LANCELOT (France), Dynagen (FRG), RTNS-I,II and Cyclotron Corporation (USA), Chalk River (Canada), OKTAVIAN and FNS (Japan). Figures 6; references 39

UDC 535.14

Frequency-Modulation Spectroscopy With Light in Compressed State

907L0070B Kiev UKRAINSKIY FIZICHESKIY
ZHURNAL in Russian Vol 34, No 12, Dec 89
pp 1800-1804

[Article by M.V. Danilenko, V.I. Romanenko, and L.P. Yatsenko, Institute of Physics, UkSSR Academy of Sciences, Kiev]

[Abstract] Lowering the noise level in frequency-modulation spectroscopy by compression of the light is considered, the effectiveness of this method being demonstrated theoretically by calculation of the modulation-dependent noise component. This is done first for positive-unilaterally modulated light and then for bilaterally modulated light, the light in each case proceeding from the modulator output through a compressing device such as a parametric amplifier and then through the test specimen to the photodetector. Into account are taken the phase shift occurring in any analyzed medium and the nonideality of a photodetector, a real photodetector being simulated by an ideal one with a beam-splitter plate in front which adds another noise mode. Inasmuch as compression modifies the modulation index, the relation between them is established and an optimum compression ratio is found to exist which will minimize the noise level. References 4.

Search for Narrow Diproton Resonances

907L0081A Moscow YADERNAYA FIZIKA in Russian
Vol 51 No 1, Jan 90 pp 135-141

[Article by L.S. Vorobyev, V.B. Gavrilov, N.A. Goryanov, Yu.G. Grishuk, P.V. Degtyarenko, Yu.V. Yefremenko, B.V. Zagreyev, S.G. Kuznetsov (deceased), S.V. Kuleshov, G.A. Leksin, N.L. Semenova, A.V. Smirnitkiy, V.B. Fedorov, B.B. Shvartsman, and S.M. Shvalov, Institute of Theoretical and Experimental Physics at State-Supervised Institute of Atomic Energy]

[Abstract] A study of narrow diproton resonances in $pA(C, Cu, Pb)$ interactions was made, a special experiment having been designed for this purpose and performed with the aid of electronic instrumentation. The carbon targets were stacks of activated-carbon pellets, the Cu and Pb targets were thin plates. Protons impinging on the target with a momentum of 7.5 GeV/s were recorded by three scintillation counters one behind the other. Secondary charge-carrying particles were recorded by a Y-form instrument with a streamer counter and four 20 cm thick scintillation counters in each of the three arms. The angles of particle tracks and the sites of particle interactions were monitored by a pair of hot-wire XY scanning cameras in each arm of the instrument, operating with or without filters for protons diverging at 70-90 angles the and for protons diverging at angles up to 180° respectively. Secondary particles were identified on the basis of their time of flight through a thick scintillator and their energy was determined on the basis of their energy dissipated in the process. Data on inelastic interactions of electrons and positrons with nitrogen and oxygen nuclei in the residual gas at the 5 GeV/s momentum level were provided by an ARGUS detector with DORIS storage rings reliably identifying protons with 0.3-1.2 GeV/s momentum at flight angles smaller than 26°. The data revealed approximately 50,000 interaction events on a C nucleus, approximately 40,000 interaction events on a Cu nucleus, and approximately 20,000 interaction events on a Pb target, interactions involving one proton or more. A statistical analysis of these data yields a very low probability of less than 10 MeV wide diproton resonances within the 1.9-2.0 GeV range of mass, but indicates a peak corresponding to a mass of 2.05- 2.12 GeV. Figures 6; references 12

Masses of Neutrinos in Left-Right Symmetry Models

907L0081B Moscow YADERNAYA FIZIKA in Russian Vol 51, No 1, Jan 90 pp 182-185

[Article by G.M. Asatryan and A.N. Ioannisyan, Yerevan Institute of Physics]

[Abstract] Radiative corrections to the Majorana mass matrix of neutrinos in left-right symmetry models such as the simplest $SO(10)$ are calculated, considering that in the $SU(2)_L \times SU(2)_R \times U(1)_{R-L}$ scheme a neutrino acquires a Dirac mass as a result of Yukawa interaction and that breaking of (B-L) symmetry imparts a Majorana mass to the right neutrino. Those corrections are small, of the $O(g^2/16\pi)$ order, so that only those to the zero element of the matrix and thus to the mass of the left neutrino are significant. A triplet of Higgs fields Φ and Δ with nonzero mean in vacuum is not included in the model but has been reconstructed from $(2 \times 2 = 3 + 1)$ doublets, to account for mass acquired by the left neutrino upon its interaction with such a triplet. The total mass of light neutrinos is calculated on this basis, with the Φ field either real or complex. The authors thank Z.G.

Berezhiani, M.N. Vysotskiy, S.G. Matinyan, and K.A. Ter-Martirosyan for helpful discussions. Figures 4; references 3

Search for Massive Neutrinos in Reactor of Rovno AES

907L0093A Moscow PISMA V ZHURNAL EKSPERIMENTALNOY I TEORETICHESKOY FIZIKI in Russian Vol 51 No 2, 25 Jan 90 pp 75-77

[Article by V.I. Kopeykin, L.A. Mikaelyan, and S.A. Fayans, Institute of Atomic Energy imeni I.V. Kurchatov]

[Abstract] Data on the mass of a heavy neutrino were obtained from its decay $\nu_H \rightarrow \nu_L + e^+ + e^-$ in the nuclear reactor of the Rovno AES [nuclear electric power station], such a neutrino having been sought in an experiment with the Rovno neutrino spectrometer. The latter contained as target a liquid organic scintillator having a 1050 dm³ large volume. A detector of light electron neutrinos recorded a $\bar{\nu}_e$ flux of $6 \times 10^{12} \text{ cm}^{-2} \cdot \text{s}^{-1}$ integral intensity, corresponding to 10^8 such neutrinos with more than 1 MeV energy. The energy spectra of events involving 1-8 MeV particles were recorded and measured during reactor operation and during reactor shutdown, whereupon the difference $S(E)$ -“effect” spectrum (E - energy absorbed in spectrometer) was constructed on the basis of these measurements. A comparison of the theoretically predicted $S(E, m_H, \sin\theta)$ -effect with that experimentally determined $S(E)$ -effect spectrum reveals constraints on both the mass and the mixing angle. The authors thank F. von Feilitzsch for the stimulating discussions (fall 1988 at the neutrino laboratory of Rovno AES). Figures 2; references 8

Phase Conjugation by Four-Wave Interaction in Molten Solution

907L0093B Moscow PISMA V ZHURNAL EKSPERIMENTALNOY I TEORETICHESKOY FIZIKI in Russian Vol 51 No 2, 25 Jan 90 pp 86-90

[Article by S.A. Viznyuk, P.P. Pashikin, A.M. Prokhorov, S.F. Rastopov, and A.T. Sukhodolskiy, Institute of General Physics, USSR Academy of Sciences]

[Abstract] Phase conjugation of a continuous-wave laser beam was for the first time achieved in a molten solution, with the dynamic phase profile remaining stable for a period of about 1 h. The experiment was performed with an LGN-404 continuous-wave argon laser operating at the 514.5 nm wave-length and a molten aqueous 60 vol percent solution of benzyl cyanide with addition of rhodamine G dye confined between two 2.7 mm thick glass plates. The laser beam was split by a cube into two beams of equal intensity. The reflected beam was again split into a pumping beam which entered the melt from one side and a reading beam which entered it from the other side, the two beams having been guided into exact opposition by an opaque plane mirror each. The beam

transmitted by the cube for recording entered the melt obliquely at a 0.052° angle to the pumping beam, appropriately guided by three successive plane mirrors. The second mirror, transmitting only 64% of incident radiation, reflected most of the returning phase-conjugate beam into a photographic camera for display of its intensity distribution and some of it onto a photo-diode for measurement of its power. The camera had been placed 2 mm behind that mirror and thus sufficiently far from scattered background light. The pumping beam and the recording beam had each a power of 60 mW, while the power of the reading beam was 120 mW. Their intensities within the interaction space were 3 W/cm^2 , 3 W/cm^2 , and 6 W/cm^2 respectively. Interference of the pumping beam and the not yet distorted recording beam produced a pattern with a 0.056 mm period and an intensity modulation with an amplitude of $(3 \times 3)^{1/2} = 6 \text{ W/cm}^2$. The photographs indicate that reflection of the recording beam upon four-wave interaction in the molten solution and its subsequent reconstruction during return passage have compensated its original large-scale fluctuations, residual distortions of the reconstructed beam being attributable to finite spatial resolution of the heterogeneous structure in the interaction space. The power of the phase-conjugate beam has been plotted as a function of time, from the instant of laser turn-on till turn-off of the recording beam and beyond, its trend over this period of time indicating a relative stability of the structure induced in the given medium and its fluctuations being evidently attributable to instability of the laser beam and mechanical vibrations of the equipment. Experimental data on the nonlinearity of recording media such as this and other ones, combined with theoretical estimates, indicate that binary solutions with a lower critical separation point are can be used as the basis for a new class of effective recording media. Figures 3; references 8

Spin Depolarization of Muons in Condensed Nitrogen

907L0094A Moscow PISMA V ZHURNAL
EKSPERIMENTALNOY I TEORETICHESKOY
FIZIKI in Russian Vol 51, No 1, 10 Jan 90 pp 7-10

[Article by V.G. Grebennik, V.N. Duginov, B.F. Kirillov, A.B. Lazarev, B.A. Nikolskiy, A.V. Pirogov, V.G. Storchak, and S.N. Shilov, Institute of Atomic Energy imeni I.V. Kurchatov and Joint Institute of Nuclear Research]

[Abstract] An experiment was performed in the phasotron at the Joint Institute of Nuclear Research concerning muon spin relaxation in condensed nitrogen. Nitrogen filling a cylindrical chamber 24 mm high and 80 mm in diameter with 0.040 mm thick mylar windows was liquified and crystallized by cooling with helium, this nitrogen chamber having been placed inside a helium cryostat with brass windows. A muon beam was injected into the nitrogen chamber along its axis and the parameters of spin precession in a transverse magnetic field of 100 Oe were measured at temperatures covering

the 8-75 K range, the nitrogen temperature being measured with a semiconductor thermometer and regulated as well as stabilized within 0.1 K by blow of gaseous helium. The results reveal a spin depolarization of the muons, the rate of this depolarization remaining fairly constant over the entire temperature range but the initial amplitude and phase of their spin precession respectively peaking and dipping at about 40 K. An analysis of the data indicates that formation of a muonium atom causes the fast depolarization of muons in condensed nitrogen, this localized muonium atom within a time shorter than the life of its excited state combining with a nitrogen molecule into diamagnetic complex ion $\text{n}_2\mu^+$ according to the exothermic reaction $\text{Mu} + \text{N}_2 \rightarrow \text{N}_2\mu^+$. Another mechanism of muon depolarization could be the $(\text{N}_2\mu^+)^* \rightarrow \text{N}_2\mu^+$ reaction where $(\text{N}_2\mu^+)^*$ denotes the excited state of a $\text{N}_2\mu^+$ ion with an unpaired electron spin. The authors thank I.I. Gurevich for interest and support, S.N. Burmistrov, I.G. Ivanter, N.V. Prokofyev, and V.G. Firsov, for discussing the results, V.A. Zhikov, V.G. Olshevskiy, and V.Yu. Pomyakushin for assisting in the experiment. Figures 1; references 6

Nuclear-Magnetic Resonance Spectra of ^{205}Tl in $\text{Tl}_2\text{Ba}_2\text{Ca}_n\text{Cu}_{n+1}\text{O}_{6+2n}$ High- T_c Superconductors With $n = 0, 1, 2$.

907L0094B Moscow PISMA V ZHURNAL
EKSPERIMENTALNOY I TEORETICHESKOY
FIZIKI in Russian Vol 51 No 1, 10 Jan 90 pp 32-34

[Article by N.Ye. Alekseyevskiy, G.M. Kuzmicheva, A.V. Mitin, V.I. Nizhankovskiy, Ye.G. Nikolayev, and Ye.P. Khlybov, Institute of Problems in Physics, USSR Academy of Sciences]

[Abstract] A study of $\text{Tl}_2\text{Ba}_2\text{Ca}_n\text{Cu}_{6+2n}$ superconductors with $n = 0, 1, 2$ was made in search of possible structural distortions such as atoms of one kind in positions of atoms of another kind, nuclear-magnetic resonance spectra of ^{205}Tl in these compounds being for this purpose recorded with a pulsed NMR-spectrometer by the spin echo method (amplitude of spin echo signal depending on magnetic field intensity) at a frequency of 22,150 kHz. Specimens were synthesized at $840\text{-}860^\circ\text{C}$ in air within a period 2 h period and then rapidly cooled, their composition being subsequently verified on the basis of x-ray diffraction analysis. Their critical superconducting transition temperature and both a,c lattice parameters were determined on the basis of magnetic susceptibility measurements. An analysis of the data, particularly of the asymmetric Tl-1 and Tl-2 lines corresponding to Tl atoms in the Tl-O layers and in other positions respectively, indicates a partial replacement of Ca by Tl with resulting appreciable changes in the properties of the material. The authors thank I.A. Kuzmin for assistance in setting up the NMR-spectrometer and S.V. Verkhovskiy for providing the results of another study prior to its publication as well as for helpful discussions. Figures 1; table 1; references 9

UDC 539.184

Relativistic Polarization Potential of Multi-Electron Atom

907L0119A Tomsk IZVESTIYA VYSSHIKH
UCHEBNIKH ZAVEDENIY: FIZIKA in Russian
Vol 33 No 1, Jan 90 pp 5-9

[Article by A.V. Glushkov, Odessa Institute of Technology imeni M.V. Lomonosov]

[Abstract] An analytical expression for the effective potential of two-particle interaction in a multi-electron atom is derived which includes the contribution of exchange-polarization diagrams in the second-order perturbation theory in the Thomas-Fermi approximation rather than exactly. Two kinds of such diagrams are involved here, three with and four without Hartree-Fock inserts. The contribution of those with inserts can be compensated exactly in any-order perturbation theory, while among the four diagrams without inserts there are two ladder diagrams, including an exchange diagram, whose contributions to the energy can be fully accounted for in the zeroth-order perturbation theory and two polarization diagrams which represent multiparticle effects. The direct polarization diagram, which describes polarization interaction of two electrons or vacancies in a polarizable medium, is calculated first and then the exchange polarization diagram is calculated analogously. The coefficient in front of the sum of integrals is by the Gauss method rather than the Thomas-Fermi method, assuming that one of the two particles is positively charged and pinned to the nucleus. The resulting polarization potential in this new form including its exchange part does not depend on the dipole and quadrupole polarizabilities of the atom shell so that they do not need to be calculated. Figures 2; references 18

UDC 530.145

New Exact Solutions to Schroedinger Equation Based on Finite-Dimensional Matrices

907L0119B Tomsk IZVESTIYA VYSSHIKH
UCHEBNIKH ZAVEDENIY: FIZIKA in Russian
Vol 33 No 1, Jan 90 pp 17-23

[Article by O.B. Zaslavskiy, Kharkov State University imeni A.M. Gorkiy]

[Abstract] New exact solutions to the Schroedinger equation are found which apply only to the part of the energy spectrum associated with spin and thus finite-dimensional systems. Under consideration is the difference equation with real coefficients $(\omega_0 - \epsilon_0)a_0 + p_s a_{s-1} + r_{s+1} a_{s+1} = 0$. Then, assuming that the matrix elements of all coefficients in this equation are complete second-degree polynomials and upon introduction of the generating function $\Phi(\varphi) = \sum a_s e^{is\varphi}$ over all s , a second-order differential equation of the Schroedinger kind is obtained by multiplication that difference equation by $e^{is\varphi}$ and subsequent summation. This equation is solved

for the case of finite series representing function $\Phi(\varphi)$ so that s varies within a finite range from s_1 to s_2 , or from $-S$ to $+S$ (S being an integer or half-integer). Most simple explicit solutions are found when $S = 3/2$, explicit exact solutions when $S = 2$ being found only for odd states. These solutions are compared with the known exactly solvable limiting models with $J = S$, $S \rightarrow \infty$, and $\beta \rightarrow 0$ so that $\beta S^2 = -\gamma_0 = \text{constant}$ or with $J \rightarrow \infty$ and $\beta \rightarrow 0$ so that $\beta J = B = \text{constant}$ when S is fixed. The natural generalization would be coefficients in the form of matrices with up to five diagonals, no other matrices yielding potentials with exact solutions by this method. References 12

UDC 539.3

Solution of One-Dimensional Problem in Nonlinear Theory of Elasticity With Structured Shock Wave

907L0116A Kiev PRIKLADNAYA MEKHANIKA
in Russian Vol 26 No 1, Jan 90 pp 103-108

[Article by A.A. Burenin and Yu.A. Rossikhin, Voronezh Institute of Construction Engineering]

[Abstract] The system of equations of wave propagation through an isotropic elastic medium is formulated in Euler variables as a one-dimensional nonlinear problem of elasticity in a rectangular Cartesian system of coordinates, assuming that both the velocity function $v[x(t)]$ and the stress function $[s(x)(t), t]$ are expandable into power series in time t . It is then reduced to a single dimensionless equation, after stress has been eliminated from two of the original ones. This equation is solved by the perturbation method with a small parameter and asymptotic expansions. Viscosity is assumed to be zero-everywhere except within a thin layer around the wave-front, where it is very low. While the small parameter can be ignored for external asymptotic expansions, the space variable must be rescaled for internal asymptotic expansions. As the viscosity vanishes, the solution becomes that of a structures shock wave. Figures 1; references 9

UDC 533.6.013.42

Constructing Mathematical Model of Adaptive Anti-Flutter System

907L0116B Kiev PRIKLADNAYA MEKHANIKA
in Russian Vol 26 No 1, Jan 90 pp 113-119

[Article by B.O. Kachanov, S.I. Ovcharenko, and A.T. Ponomarev, Military Aircraft Engineering Academy, Moscow]

[Abstract] A linear mathematical model of an anti-flutter system for aircraft is constructed on the basis of an approximate finite-dimensional mathematical description of perturbed aircraft motion and its stability analysis in accordance with the Mikhaylov's aeroelasticity criterion. For simplification of the iterative calculation process, the aerodynamic and kinematic parameters are assumed to vary harmonically at the stagnation point.

To make the system adaptive, the model includes algorithms of identification, estimation, and optimal control based on that simplified aeroelasticity model. Practical application is demonstrated on suppression of symmetric flutter of a hypothetical transport plane during depletion of fuel, the fuel being carried in tanks under the wings and the rudders with a surface area constituting one quarter of the aileron surface are extending

almost to the tip of the wings. Three coefficients most sensitive to fuel depletion have been selected for adaptive control by sensitivity analysis of the critical flutter velocity and frequency to variation of coefficients in the model equation, the other coefficients assumed to remain constant at their design values corresponding to the basic plane load. Figures 5; references 10

UDC 681.4

Present Status and Outlook for Development of Optical Scanning Microscopy

907L0109A Moscow IZVESTIYA AKADEMII NAUK
SSSR: SERIYA FIZICHESKAYA in Russian Vol 54
No 2, Feb 90 pp 208-212

[Article by V.G. Dyukov and Yu.A. Kudeyarov]

[Abstract] Design and performance characteristics of two optical scanning microscopes, the confocal one and the near-field one, are overviewed from the standpoint of their advantages over a plain optical microscope and coordination with a scanning electron microscope. Their advantages include a higher lateral resolution, immunity to the effect of diffraction on the illuminance distribution over the light probe, possibility of layer-by-layer imaging of an object (in a confocal microscope) with a submicrometer depthwise resolution, possibility of operation in the beam-induced current mode, and adaptability without major modifications to operation with lasers covering the entire spectrum from infrared through visible to ultraviolet light. Optical scanning microscopes can, moreover, be combined with automatic quantitative image processing. The theory of optical scanning microscopes is based essentially on Fourier optics and on the contrast-frequency characteristic. While the resolution of a confocal scanning microscope exceeds Rayleigh's diffraction limit in a plain microscope, Lukosh's rule of an invariant SW_0 product (S - area of useful object field, W_0 - width of spatial frequency passband in two dimensions) is more easily satisfied in a near-field scanning microscope. An analysis of the trends indicates several areas of research and development activity, aimed not only at perfecting the illuminance distribution and the contrast-frequency characteristic but also at improving the induced-current mode of operation, at widening the frequency range and refining the time resolution for the stroboscopic mode of operation, also at extending the usefulness of optical scanning microscopes to study of semiconductor and superconductor materials involving measurements which require distortionless imaging of transmittance or reflectance distributions. Figures 2; references 10

Recording Femtosecond Pulses of Ultraviolet Light by Two-Photon Luminescence of CsI:Na Crystal

907L0118A Leningrad PISMA V ZHURNAL
TEKHNICHESKOY FIZIKI in Russian Vol 16 No 3,
12 Feb 90 pp 28-31

[Article by R.G. Deutsch, F. Noack, V. Rudolph, and V.Ye. Postovalov]

[Abstract] A very sensitive simple method of recording and measuring femtosecond pulses of ultraviolet light emitted by excimer or dye lasers is proposed, namely by two-photon luminescence activated in crystals which have a wide energy gap. The method was tested with a

CsI:Na crystal on a passively mode-locked dye laser emitting 308 nm light in pulses of 200 μ J energy and about 30 fs duration. Such a crystal was selected not only because of its 6.2 eV energy gap, wider than $h\nu_e$ and narrower than $2h\nu_e$ without an activator absorption band within the $h\nu_e$ range, and because of its 0.3 high quantum yield with the 420 nm activator emission band within the recording range but also because of its high resistance to two-photon radiation. Measurements made with the aid of four mirrors, two lenses, a set of light filters, and three photodiodes have yielded the pulse autocorrelation function and the dependence of two-photon luminescence on the excitation pulse intensity, also the two-photon absorption coefficient needed for correction of the autocorrelation readings. The luminescence extinction time was 300 ns and the absorption coefficient varied over the $(2.5-6.5) \times 10^{-9}$ cm/W range. The total luminescence intensity was found to depend on the excitation pulse energy quadratically below 32 μ J and linearly above 32 μ J. The time resolution of this recording and pulse duration measuring method was found to be better than 1 fs with a strongly Na-activated CsI crystal. Figures 2; references 7

Formation of Fractal Structures During Explosion

907L0118B Leningrad PISMA V ZHURNAL
TEKHNICHESKOY FIZIKI in Russian Vol 16 No 3,
12 Feb 90 pp 42-46

[Article by A.P. Yershov, A.L. Kupershtokh, and V.N. Kolomiychuk, Institute of Hydrodynamics, Siberian Department, USSR Academy of Sciences, Novosibirsk]

[Abstract] An experimental study of ultrafine-disperse diamond powder was made, the fractal dimensionality of clusters being measured to monitor their formation during explosion with attendant exhalation of free carbon. Measurements were made by the method of low-angle ($7^\circ < 2\theta < 7^\circ$) x-ray scattering with a 0.154 nm x-radiation source. The readings fit a log-log curve consisting of three successively steeper linear segments and thus indicate a two-stage rather than direct growth of clusters, atoms first aggregating into compact particles and these then forming clusters. The fractal dimensionality $D = 1.9$, approximately, corresponds to the compact-cluster aggregation stage, the characteristic dimension of a particle and of an aggregate being 3 nm and 20 nm respectively according to estimates based on the two boundaries of the fractal range as well as on the model of two particles merging upon collision. Formation of aggregates by cluster-cluster association is analyzed qualitatively only, remaining solitary particles and solitary clusters being regarded as relicts of the chemical reaction. The authors thank A.I. Lyamkin and V.A. Molokoyev for supplying the experimental specimens, A.M. Staver, V.F. Anisichkin, and I.Yu. Malkov for helpful discussions, and V.M. Titov for interest. Figures 2; references 8

UDC 535.34:621.315.592

Nonlinear Optical Absorption of Light in KS-19 Glass

907L0117A Kiev UKRAINSKIY FIZICHESKIY
ZHURNAL in Russian Vol 35 No 2, Feb 90 pp 200-205

[Article by N.R. Kulish, V.P. Kunets, and M.P. Lisitsa, Institute of Semiconductors, UkSSR Academy of Sciences, Kiev]

[Abstract] In search of materials for optical computers, inclusion of semiconductor microcrystals in a thin glass matrix is considered as means of ensuring adequate mechanical strength as well as high switching speed based on absorptive or dispersive bistability. Nonlinear absorption of light in KS-19 glass containing hexagonal $\text{CdS}_x\text{Se}_{1-x}$ microcrystals was studied in an experiment with a dye laser emitting visible light within a 0.05 nm wide band in pulses of 20 ns duration. The transmission coefficient for 674.3 nm, 668.7 nm, 660.0 nm light was measured with the intensity of light varying over the 4×10^3 - 4×10^8 W/cm² range. The thus obtained $T(I_0)$ curves do fit the model applicable to a two-level medium, but are shown to be consistent with the dynamic effect in a medium with two kinds of centers according to the Burstein-Moss model. The validity of this interpretation is based on results of electron-microscope examination and electron-diffraction analysis, which indicate that $\text{CdS}_x\text{Se}_{1-x}$ microcrystals have a wurtzitic structure and are random distributed in the glass. An explanation for nonlinear absorption of light is accordingly found in hydrostatic compression of these microcrystals by the glass during its solidification and attendant shrinkage in the founding and annealing process, its coefficient of linear thermal expansion being much larger than that of CdS and CdSe. Precise iterative calculation of pressure P as a function of x , as CdSe is increasingly replaced by CdS, yields a pressure changing from 4.65 kbars when $x = 0$ to 6.46 kbars when $x = 1$ and thus remaining far below the 30 kbars at which transition of CdSe and CdSe from wurtzitic to halitic structure occurs. Figures 2; tables 1; references 27

UDC 535:621(3.038+376.2+373.44)

Microsecond-Pulse Nd-Glass Laser With Monopulse Duration Control

907L0117B Kiev UKRAINSKIY FIZICHESKIY
ZHURNAL in Russian Vol 35 No 2, Feb 90 pp 209-213

[Article by B.V. Anikev and V.V. Krutyakov, University of Volgograd]

[Abstract] A technological pulsed Nd-glass laser with power stabilizing external negative feedback has been built for applications such as micro-welding which require flat-top laser monopulses with duration control. Both beginning and ending an emission monopulse are controlled by Q-switching an electrooptic shutter which

operates on the basis of the longitudinal Pockels effect. Precise control of the pulse start is achieved by suppression of acoustic waves generated upon impact excitation of the shutter by the piezoelectric effect, this excitation being effectively prevented by damping the laser crystal so that quasi-continuous pulse emission becomes attainable with the maximum pulse duration determined by duration of the pumping pulse. The optical cavity, optically 90 cm long, is formed by two mirrors with 1.0 and 0.40 reflection coefficients respectively. A diaphragm reducing the diameter of the laser beam to 4 mm protects the shutter fixture against burns. A unique feature of the shutter is an additional polarizer, a Brewster stack of nine plates, maximizing the contrast. Feedback signals are generated by a coaxial photocell. The laser was tested for performance, including dependence of laser plus feedback kinetics on the rise time of Q-switching pulse and reliability of transition to quasi-continuous monopulse emission. Figures 2; references 7

Breakup of Femtosecond Pulses During Amplification in Er^{3+} -Doped Single-Mode Optical Fibers

907L0113A Moscow PISMA V ZHURNAL
EKSPERIMENTALNOY I TEORETICHESKOY
FIZIKI in Russian Vol 51 No 3, 10 Feb 90 pp 121-124

[Article by A.B. Grudinin, Ye.M. Dianov, D.V. Korobkin, A.Yu. Makarenko, A.M. Prokhorov, and I.Yu. Khrushchev, Institute of General Physics, USSR Academy of Sciences]

[Abstract] Amplification of femtosecond solitons by stimulated Raman scattering (SRS) in Er^{3+} -doped optical fibers is considered, fibers doped with rare-element ions acquiring the characteristics of an active laser medium and the duration of femtosecond solitons being comparable with the transverse-relaxation time for the $^4\text{I}_{13/2}$ and $^4\text{I}_{15/2}$ transition in a Er^{3+} ion. An experiment was performed with an SRS soliton generator and a 35 m long fiber. The soliton generator consisted of a YAG:Nd³⁺ laser with simultaneous mode locking and Q-switching. The fiber operated with zero chromatic dispersion at the 1.32 μm wavelength. Spectral characteristics were measured with a reticular monochromator and the time characteristics with an intensity autocorrelator by the zero-background method, the resolutions being not worse than 0.5 nm and 15 fs respectively. Solitons of 80 fs duration within the 1.54 μm radiation band were injected into the fiber, the latter having a 0.1% Er-ion content and being pumped with second-harmonic radiation from a mode-locked YAG:Nd³⁺ laser. With an average laser emission power of 2 W, the pumping efficiency was 50% and the signal injection efficiency varied over the 4-40% range. For a study of the pulse propagation dynamics within the Stokes region, the duration of solitons was lengthened to 120 fs by addition of a 100 m long passive fiber and signal pulses were made to pass through a 70 cm long segment of it before entering the activated one. The results of measurements

indicate two stages of the amplification process. A non-linear pulse first acquires energy without changing its time characteristics, while frequency pulling and structural stabilization avert its breakup into "color" solitons till some threshold energy level much higher than the energy of the fundamental soliton is reached. As this level is exceeded, the pulse begins to contract till it breaks up and a long-wave wing shifting into the Stokes region owing to stimulated Raman self-scattering appears in its spectrum. This interpretation of the experimental data is confirmed by numerical estimates. The authors thank E.A. Vanagas (Institute of Semiconductor Physics, Vilnius) for helpful discussions and D.N. Payne (University of Southampton, U.K.) for providing the activated optical fiber. Figures 3; references 6

Electron-Hole Droplets or Laser Effect in Germanium Crystals?

907L0113B Moscow PISMA V ZHURNAL
EKSPERIMENTALNOY I TEORETICHESKOY
FIZIKI in Russian Vol 51 No 3, 10 Feb 90 pp 124-128

[Article by A.A. Kipen, Institute of Physics, UkSSR Academy of Sciences]

[Abstract] It is demonstrated on the basis of three indications that the characteristics of radiation attributable to electron-hole droplets in a germanium crystal can also be interpreted by treating such a droplet as a laser. According to this model, emission of radiation follows selective amplification of spontaneous exciton luminescence by stimulated transitions in total-internal-reflection modes of the natural optical cavity resonator formed by the crystal facets. The first indication is amplification of that dominant spontaneous emission during multiple passage of light through the active region of this cavity resonator, with the maximum in the intensity spectrum $I(h\nu)$ shifting toward the maximum in the gain spectrum $G(h\nu)$ and both stabilizing within a narrow $h\nu$ range (707-712 meV) as one approaches the threshold of droplet luminescence by either lowering the initially high temperature while holding the low pumping level constant or by raising the initially low the pumping current while holding the high temperature constant. The second indication is predominance, at low temperatures, of scattering over absorption of radiation emitted by droplets. The third indication is additional weak absorption inside the cavity, detectable by laser intracavity spectroscopy and manifested by appreciable "shrinking" of the contour of the laser emission (droplet luminescence) band when the absorption line lies within that much wider band. The apparent inconsistency of the form of the droplet luminescence (laser emission) band with the exciton-exciton mechanism of inversion in the Ge exciton system is resolved is not real, inasmuch as both the form of that contour and the location of that band in the spectrum are determined not by the contour of gain curve but by the form of the absorption edge within this segment of the spectrum. Figures 3; references 10

Magnetostriction in $\text{PrBa}_2\text{Cu}_3\text{O}_{7-d}$ Single Crystal

907L0113C Moscow PISMA V ZHURNAL
EKSPERIMENTALNOY I TEORETICHESKOY
FIZIKI in Russian Vol 51 No 3, 10 Feb 90 pp 172-175

[Article by A.K. Zvezdin, A.M. Kadomtseva, A.A. Kovalev, M.D. Kuzmin, L.I. Leonyuk, N.I. Leonyuk, A.S. Markosyan, and V.N. Milov, Moscow State University imeni M.V. Lomonosov]

[Abstract] An experimental study of magnetostriction in $\text{PrBa}_2\text{Cu}_3\text{O}_{7-d}$ single crystals was made, this property being sensitive to instability of the valence of praseodymium. Rhombic crystals were grown from the melt of a nonstoichiometric solution as the latter was cooling from 1150°C to 400°C at a rate of 5°C/h. Magnetostriction was measured with a piezoelectric contact transducer in a pulsed external magnetic field of up to 75 kOe intensity. It was measured along both -a- and -b- axes, the crystal being variously oriented relative to the magnetic field. It was measured at temperatures covering the 4.2-200 K range. These measurements have yielded not only the field dependence of magnetostriction but also series of magnetostriction isotherms, the 4.2 K isotherms being characterized by an extremely strong anisotropy in both magnitude and sign of the magnetostrictive effect. One possible mechanism of magnetostriction is valence instability of praseodymium, Pr^{3+} and Pr^{4+} ions being normally at equilibrium in a $\text{PrBa}_2\text{Cu}_3\text{O}_{7-d}$ crystal. Because the magnetic characteristics of the two ions differ, their equilibrium is sensitive to change in the intensity of the external magnetic field. Because the two ions have different radii, moreover, a shift of their equilibrium causes deformation of the crystal lattice. Theoretical estimates as well as experimental data indicate that this mechanism explains the temperature-and-field dependence of magnetostriction, on the assumption that the concentration of each Pr ion in the absence of a magnetic field is very low and not temperature-dependent. The contributions of Pr^{3+} ions alone and of Pr^{4+} ions alone in magnetostriction above the Neel point are calculated in the high-temperature approximation $T \gg \mu_B H$, using the Stevens coefficient for rare-earth compounds. They are found to be also both temperature and field dependent, the much larger contribution of Pr^{3+} ions indicating predominance of trivalent praseodymium with tetravalent praseodymium existing as an impurity only. Figures 2; references 12

UDC 535.417

Accounting for Refraction in Optical Tomography

907L0079A Leningrad OPTIKA I SPEKTROSKOPIYA
in Russian Vol 67 No 6, Dec 89 pp 1353-1359

[Article by B.F. Apter and B.Ye. Kunber]

[Abstract] The problem of optical tomography, determining the spatial density distribution of a nonhomogeneous medium, is solved as an inverse problem on the

basis of perturbation theory for light rays so as to take into account their multiple refractions and resulting curvilinearity of their path. In the first-order theory the relation between the sought radial profile of the refractive index and the measured field eikonal reduces to the Radon equation, with the ordinate y_1 of a ray's entry point into the plane of measurement $x_1 = \text{constant}$ treated as a function of the ordinate y_0 of its exit point on the wavefront $x_0 = \text{constant}$, such a treatment requiring another measurement. In the second-order theory the problem reduces to an integrodifferential equation with a Radon kernel, which can be solved directly by the iteration method. The problem has been formulated in both first-order and second-order approximations, it has been solved numerically for an axisymmetrically nonhomogeneous medium so that the Radon integral equation reduces to the Abel integral one. Reconstruction of Gaussiannonhomogeneity and "annular" nonhomogeneity with and without refraction taken into account demonstrates the effectiveness of this method. Figures 4; tables 1; references 5

UDC 621.375.9

He-Ne Laser Emitting Five Lines Simultaneously

907L0079C Leningrad OPTIKA I SPEKTROKOPIYA
in Russian Vol 67 No 6, Dec 89 pp 1418-1419

[Article by Ya.M. Bondarchuk, R.M. Voznyak, and V.Ye Privalov]

[Abstract] A multicolor He-Ne laser has been developed which emits simultaneously five lines within the visible range of the spectrum. Its approximately 2 m long cavity is formed by two spherical mirrors, a 19-layer coating on each ensuring higher than 0.99 reflection coefficient for 590-710 nm light with a 3,390 nm transmission window. This cavity is almost fully occupied by the active medium in a bipartite cell with a common cathode between its two arms. Cavity and active medium have been so matched as to prevent suppression of emission at 640 nm, 635 nm, 629 nm, and 612 nm wavelengths by the emission of 633 nm radiation. The total multicolor emission power with a 72-76 mA current through the cathode is 4.8 mW, split between the five lines in a $P(640):P(635):P(633):P(629):P(612) = 0.4:0.1:1:0.1:0.5$ ratio. Separate emission of each line is achieved by replacement of one mirror with a Littrow prism. Figures 1; references 4

UDC 535.343.2+535.344

Vacuum-Ultraviolet Characteristics of New Fluoride Matrix

907L0101A Moscow DOKLADY AKADEMII NAUK
SSSR in Russian Vol 310 No 1, Jan 90 pp 72-74

[Article by K.M. Devyatkov, O.N. Ivanova, K.B. Seyranyan, S.A. Tamazyan, and S.P. Chernov, Moscow State University imeni M.V. Lomonosov]

[Abstract] An experimental study of the new matrix material for active media of solid-state lasers KY_3F_{10} was made, this material being transparent to vacuum-ultraviolet light when activated by trivalent ions of a rare-earth element such as Er^{3+} . Pure single crystals were grown by the Stockbarger-Bridgman method from the melt of extra-pure $KF \cdot HF$ and 99.995% pure YF_3 in a graphite container in a graphite resistance furnace, the fluoridizing atmosphere being produced by thermal decomposition of teflon, the melt also including 99.999% pure ErF_3 for preparation of activated single crystals. Disks 1 mm thick and 10 mm in diameter were cut for the experiment. Their transmission spectra were measured with a VMR-2 monochromator at room temperature. Their luminescence spectra were measured with two monochromators crossing each other, a VMR-2 and a DFS-29, at room temperature and in a cryostat at liquid-nitrogen temperature. The transmission spectrum of intrinsic KY_3F_{10} crystals reveals a wide transmission range apparently ending at the 132 nm ($75,760 \text{ cm}^{-1}$) absorption edge, actually at a shorter wavelength if allowance is made for residual absorption owing to an imperfect surface finish. The absorption spectrum of $KY_3F_{10} : Er^{3+}$ (4 atom.% Er^{3+}) crystals consists of weak lines within the 50,000-55,000 cm^{-1} band attributable to 4f-4f transitions in the Er^{3+} ion and a wider band with a peak at the 60,850 cm^{-1} frequency, the intensity of absorption in this band being too high for 4f-4f transitions but too low for 4f-5d transitions. The luminescence spectrum of $KY_3F_{10} : Er^{3+}$ crystals excited by 158 nm ($63,300 \text{ cm}^{-1}$) consists of a sharp peak about the 169 nm wavelength, this peak corresponding to the lower excited 5d-state of the Er^{3+} ion at room temperature and only narrowing from a 2000 cm^{-1} wide to a 1300 cm^{-1} wide as the temperature drops to liquid-nitrogen levels. Article was presented by Academician N.D. Devyatkov on 25 June 1988. Figures 2; references 8

Origin of Residual Surface Resistance of Ceramic High-Temperature Superconductors

907L0104B Leningrad PISMA V ZHURNAL
TEKHNICHESKOY FIZIKI in Russian Vol 16 No 1,
12 Jan 90 pp 77-79

[Article by N.V. Fomin, Institute of Engineering Physics imeni A.F. Ioffe, USSR Academy of Sciences, Leningrad]

[Abstract] Apparently paradoxical results of an experiment revealing a residual surface resistance of a ceramic high-temperature superconductor in a microwave field at a temperature near absolute zero are explained on the basis of the Bardeen-Cooper-Schrieffer theory, considering that the excited states are in this theory separated from the ground state by the energy gap. Their along with the heat dissipation associated with them accordingly decrease exponentially, therefore also does the surface resistance, as the temperature approaches absolute zero. The paradox is resolved by taking into account losses in the natural mode of the microwave resonator due to diffuse diffractive scattering of this mode by randomly

oriented anisotropic macrograins of the ceramic material. Quantitative theoretical estimates validating this interpretation of those experimental results are made on the basis of a simple model with only two equiprobable orientations of grains whose C-axis either runs to the perpendicularly to the surface parallel to the Z-axis or runs parallel to the X-axis in the Cartesian system of coordinates. Reflection of a normally incident wave by the surface of a ceramic superconductor is analyzed on this basis, assuming that the electric field of this wave lies in the XZ-plane and penetrates a grain of either orientation to a depth much smaller than the grain diameter. A single crystal of a high-temperature superconductor is considered next, its optical anisotropy being recognized as resulting principally from interaction of Cooper-pair electrons and the anisotropic crystal field and accounted for by extending the London equation to the effective electron tensor mass. References 2

Experimental and Theoretical Study of Forces and Spatial Resolution in Atomic Force Field Microscope

907L0083A Leningrad ZHURNAL TEKHNIЧЕСКОY FIZIKI in Russian Vol 60 No 1, Jan 90 pp 141-148

[Article by Yu.N. Moiseyev and V.I. Panov, Department of Physics, Moscow State University imeni M.V. Lomonosov, V.M. Mostepanenko and I.Yu. Sokolov, All-Union Scientific Research Institute of Metrology imeni D.I. Mendeleev]

[Abstract] An approximate method of calculating the Van der Waals molecular interaction forces in the "tip above plane surface" configuration of an atomic force field microscope is proposed, such a microscope featuring a high spatial resolution which approaches that of a scanning tunneling microscope and being useful for study of dielectric as well as conductor surface microreliefs. This method is based on a simple theoretical relation describing the distance dependence of the Van der Waals interaction force. The tip is assumed to be a paraboloid of revolution. Interaction of individual tip material molecules and plate material molecules is a Lennard-Jones repulsion when the distance from tip to plate is of the order of 0.1 nm and a nonretarding Van der Waals (London) attraction when the distance between molecules exceeds 0.4 nm up to wavelengths within the absorption spectra of the two materials. The method, an adaptation of the Casimir-Polder method, replaces separation of variables in the wave equation and derivation of the Green function for a photon in the medium with additive summation of nonadditive interactions involving individual atoms and subsequent diminution of the thus obtained potential constant by an appropriate factor representing degree of nonadditivity. The resolution of an atomic force field microscope in the direction normal to the surface is then calculated according to the Manley-Rowe relation. The results of an experiment fit very closely on that theoretical force-distance curve, of an experiment, measurements having been made on a scanning atomic force field microscope

with a dielectric tip mounted on the free end of an initially horizontal cantilever beam above a plate and under a needle-electrode. Deflection of the free beam end and thus displacement of the tip was indicated by change in the magnitude of the tunneling current. Such a microscope was subsequently used for reliable and informative study of the surface structure of sapphire single crystals. The authors thank L.V. Keldysh for support and G.I. Salister (?) for stimulating discussions. Figures 5; references 22

Factors Limiting Duration of Pulsed Electron Beam Formed Along Climbing Magnetic Field in High-Current Diode

907L0083B Leningrad ZHURNAL TEKHNIЧЕСКОY FIZIKI in Russian Vol 60 No 1, Jan 90 pp 133-140

[Article by V.G. Kovalev, O.L. Komarov, O.P. Pecherskiy, Yu.M. Savelev, K.I. Tkachenko, and V.I. Engelko]

[Abstract] Formation of pulsed relativistic high-current electron beams is analyzed, maximum pulse duration and high beam stability being attained by placing the diode in longitudinally climbing magnetic field and suppressing reverse flow of electrons. The pulse duration is determined by either the cathode-anode span or the cathode-collector span, but a shorter duration under higher voltages has been noted and attributed to the breakdown characteristics of diodes in a nonuniform magnetic field. An experimental study of this problem was made, with the accelerating gap placed in the upper part of the cylindrical insulator tube above the beam transport channel and the surrounding it solenoid for a minimization of leakage currents and with a circuit of homogeneous artificial lines serving as a Marx-Arkadyev generator of high-voltage pulses. The results of measurements have revealed that the micropervance of such a diode first increases slowly as the pulse duration increases to about 10 μ s, then remains almost constant as the pulse duration increases to about 40 μ s, and then increases again but much faster as the pulse duration increases further. The probability of unstable diode operation was found to increase, with an attendant shortening of the beam pulse, as the voltage was raised above 200 kV or as the magnetic induction at the cathode was dropped below 1.5 kG. This decrease of the pulse duration is evidently caused by a fast rise of both anode and collector leakage currents up to their respective maximum levels corresponding to a short circuit across the voltage pulse generator. A theoretical analysis finds an explanation of this behavior in oscillations of electrons along the climbing magnetic field within the cathodic region, the anode leakage current increasing as a result and causing the anodic plasma to expand so that beam pulse duration simultaneously decreases as a consequence. Figures 7; references 18

**Limiting Pulse Signal in NbN-Si Structure:
Superconductor Film on Substrate**

907L0083C Leningrad ZHURNAL
TEKHNICHESKOY FIZIKI in Russian Vol 60 No 1,
Jan 90 pp 218-222

[Article by Ye.F. Gatsura, A.B. Kozyrev, and T.B. Samoylova, Leningrad Institute of Electrical Engineering imeni V.I. Ulyanov (Lenin)]

[Abstract] An experimental study was made concerning the effect of electromagnetic pulses on an NbN-Si structure consisting of an NbN-film microstrip and a Si single crystal as substrate. The substrates were 0.350 mm thick KEF-1.0 silicon wafers with [111] orientation, 5 mm wide and 8 mm long. Some of them were oxidized for expulsion of doping impurities, necessary of subsequent NbN resistance measurements. On these SiO₂ substrates as well as on the Si substrates were deposited 10-200 nm thick NbN films, by ionplasma getter sputtering of a niobium target in an Ar+ N₂ atmosphere at 750°C and at 400°C. Their width was also varied, photolithographically, over the 70-200 μm range with the length of each set at 2 mm. The static current-voltage characteristics of the substrates alone were measured at temperatures ranging from 20 K to 4.2 K. The static current-voltage characteristics of NbN films on SiO₂ substrates and on Si substrates were measured at 4.2 K. Measurements were also made for determining the dependence of the critical superconducting transition temperature and of its fluctuation range, also of the R_{300K}/R_{17K} NbN resistance ratio, on the thickness of 750°C NbN films. The results indicate that such structures behave like linear-nonlinear limiters when the NbN film switches from superconducting to normal state with attendant impact ionization of the silicon substrate acting as a discharger. They were accordingly tested in a transmission line for pulse response characteristics such as sensitivity, speed, and linear-nonlinear behavior modes. Figures 5; references 6

UDC 621.378.325

**Increasing Speed of Adaptive Control of
Light-Beam Front in Multidither Algorithm, Part
2: Practical Implementation of Algorithms**

907L0089A Tomsk OPTIKA ATMOSPHERY in Russian
Vol 3 No 1, Jan 90 pp 74-78

[Article by V.A. Trofimov, Moscow State University imeni M.V. Lomonosov]

[Abstract] Controlling the light-beam front in multidither coherent adaptive optical techniques without involving a gradient method is considered, optimum rules of varying the control constants having been proposed earlier and now being tested for practical feasibility. These include an algorithm for estimating the effectiveness of compensation of nonlinear distortions on the basis of the peak intensity or power functional and, when the receiver cannot be easily located, a modification of this algorithm which features a low probability of stochastic adaptation modes. When the

optimal rules are not implemented, then iterations for determining the optimum light-beam front is a process converging as a geometrical progression. Acceleration of the convergence requires algorithms other than those of gradient methods, the Newton method ensuring quadratic convergence and thus being preferable. Increasing the response speed of multichannel adaptive optics is problematic, a flexible mirror requiring not only actuators for focusing the light beam but also separate sets of actuators for eliminating each type of aberration. Damping is desirable and attainable by means of constraints on shape distortion, attendant regularization of the adaptation process making the minimizable functional convex and its dependence on the optimizable parameters as a single-valued one. References 8

UDC 535.343.4:523.035.338

**Multiline Representation of Integral Radiation
Absorption in Molecular Bands**

907L0089B Tomsk OPTIKA ATMOSPHERY in Russian
Vol 3 No 1, Jan 90 pp 79-82

[Article by A.G. Ishov and N.V. Krymova, Scientific-Industrial Association 'Tayfun', Obninsk]

[Abstract] Multiline representation of radiation absorption in molecular vibrational-rotational bands is described and examined, such a band consisting of generally n overlapping lines each one of which has its intensity S , half-width γ , center frequency ν_0 , and profile $\alpha(\nu_0 - \nu)$ (α - absorption coefficient). In order to calculate the integral radiation absorption, it is necessary to establish an equivalent width of the band. The procedure is demonstrated for an optically homogeneous medium with a small overlap of lines. It essentially involves differentiation the frequency spectrum ν and subsequent two summations, the sum of integral terms which take into account the generally different optical thickness τ for the center frequency of each line being subtracted from the sum of the equivalent widths of all lines in a band. The resulting expression, a difference of two sums, is asymptotically exact, its first sum representing the equivalent band width in the approximation of nonoverlapping lines. For atmospheric gases second sum amounts to a small correction which can be readily estimated from the physical properties of those gases. The exact multiline representation is applicable to any band or combination of bands including those of optically nonhomogeneous media. In that case the $\tau\alpha(\nu_0 - \nu)$ terms must be replaced with corresponding integrals of the molecule concentration profile over the absorption length. Numerical calculations have been made in the approximation of a Lorentz profile with the lines in a band arranged in the order of decreasing optical thickness, numerical integration having been performed on a computer using the QVANC8 adaptive quadrature subroutine till the final relative error had been reduced to 1×10^{-7} . Figures 1; references 7

UDC 535.343

Effect of Paramagnetic Impurities on Dynamics of Magnetic Fluxes in Superconductors907L0080A Kiev UKRAINSKIY FIZICHESKIY
ZHURNAL in Russian Vol 35 No 1, Jan 90 pp 131-135

[Article by Yu.I. Gorobets, A.N. Kuchko, and V.I. Finokhin, Donetsk University]

[Abstract] The effect of paramagnetic impurities on the redistribution of magnetic fluxes in a magnetic superconductor with a system of noninteracting paramagnetic ions is analyzed theoretically in terms of electron spin and magnetic flux interaction rather than generation of normal currents, the spin-flux interaction mechanism also being the stronger one in ceramic high-temperature superconductors with a low-conductivity normal phase and in thin-film superconductors with strong size effects. A plane N-S interphase boundary is assumed to propagate through the material so that two magnetic fields act on the paramagnetic ions: a constant magnetic one produced by their exchange interaction with the magnetic subsystem in the superconductor and a variable one associated with penetration of the external magnetic field into the superconductor. This variable magnetic field and the velocity of the interphase boundary are at right angles to each other, the intensity of this magnetic field varying in the direction of the velocity and also as a function of time. Its distribution over the moving boundary is assumed to remain static over a wide range of boundary velocities. Following a superposition of both internal magnetic fields, interaction of a solitary paramagnetic ion with the resultant magnetic flux and the magnetic subsystem in the superconductor is described by the corresponding interaction Hamiltonian. The energy transfer to a paramagnetic ion upon crossing the interphase boundary is calculated in the approximation of slow ion relaxation, assuming a Boltzmann energy distribution of paramagnetic ions prior to phase transition (time $t = -\infty$). The energy transfer to the entire system of paramagnetic ions, proportional to their concentration and to the velocity of the interphase boundary, is then calculated in an asymptotic form which differs for low temperatures and for high temperatures. The energy lost by a solitary Abrikosov vortex moving at a constant velocity in a type-II superconductor is then calculated on the basis of the Clem model, whereupon the contributions of electromagnetic and paramagnetic losses to the energy dissipation function are compared relative to the Joule heat produced by normal currents around the vortex center. Estimates are made for $\text{YBa}_2\text{Cu}_3\text{O}_{4-x}\text{Fe}^{3+}$ ceramic, the energy transfer here depending on the Fe-ion concentration and on the technology of material preparation as well as on the temperature. References 12

UDC 530.145

Phenomenological Theory of Phase Transitions to Nonhomogeneous Noncommensurate Phase With Superconducting Current907L0098A Moscow DOKLADY AKADEMII NAUK
SSSR in Russian Vol 310 No 3, 30 Jan 90 pp 599-603

[Article by Academician A.M. Prokhorov, A.Ya. Braginskiy, Yu.M. Gufan, and Ye.G. Rudashevskiy, Institute of General Physics, USSR Academy of Sciences, Moscow]

[Abstract] A phenomenological theory is constructed to describe structural transition of a crystal from a plain highly symmetric phase to a less symmetric one with small-scale but still macroscopic nonhomogeneity, such a transition occurring necessarily as an intermediate one when direct transition of the second kind from one homogeneous crystalline phase to another is not possible. The small group G_k is assumed to remain unchanged while the $k(x)$ vector (x -macroscopic space coordinate characterizing the volume of a crystal sufficiently macroscopic for being associated with density of the Landau nonequilibrium potential) varies within the Brillouin zone along some axis z . As a specific example are considered 123-phase high- T_c superconductor compounds such as $\text{Y}(\text{RE})\text{Ba}_2\text{Cu}_3\text{O}_{7-d}$ with an approximately perovskitic primitive crystal structure, the cubic crystal being trebled along one of the fourth-order axes and the corresponding $G_k = C_{3v}$ group being retained for all vectors $k = (1/3)b_3 + \mu b_3$ for all values of μ within the Brillouin zone. While trebling of such a crystal is possible only because the real order parameter is a multicomponent one with translatory properties characterized by a vector $k_1 = (1/3)b_3$ star, an "effective" two-component order parameter is considered so that structural changes of such a crystal can be attributed to the other component. Then, ignoring the noncommensurate order parameter ξ_k , the tetragonal phase and the orthorhombic phase then ought to be regarded as two tetragonal antistructural phases or, with that parameter included, the "truly" orthorhombic phase ought to be regarded as an intermediate one between two antistructural tetragonal ones. These conclusions will agree with experimental evidence, if the superconducting phases are identified as phases with nonuniform charge distribution owing to a jump of ξ_k . Figures 1; references 12

UDC 535.31+539.21

Nonuniqueness of Autowave Modes of Switching Wave Propagation Through Media With Memory907L0098B Moscow DOKLADY AKADEMII NAUK
SSSR in Russian Vol 310 No 3, 30 Jan 90 pp 603-606

[Article by S.L. Sobolev, Institute of Chemical Physics, USSR Academy of Sciences, Chernogolovka (Moscow Oblast)]

[Abstract] Autowave modes of switching wave propagation through distributed active with memory are considered, parabolic equations adequately describing such

modes in media at local thermodynamic equilibrium but not when they propagate at a high velocity such as in superconductors and in solids with a low threshold for excitation of heat sources or at low temperatures. In those case relaxation of the medium to local thermodynamic equilibrium needs to be included and the heat transfer is determined not by the instantaneous gradient of the thermodynamic potential but by the history of the process. An equation of heat conduction which includes this factor as well as the law of energy conservation is derived on the basis of corresponding integral equations for the thermal flux and the internal energy. Further analysis reveals that relaxation appreciably influences the heat transfer processes and thus also the autowave modes of switching wave propagation. The second derivative of temperature with respect to time indicates a wave mode of heat transfer while the first derivative of the source function with respect to time indicates a role of the "inertia" of heat sources in fast heat transfer processes. When the velocity of switching waves is much higher than the velocity of heat propagation in the medium, then either phase waves or athermal autowaves can appear. Either one autowave mode or three can exist in the latter case, owing to thermal memory of the medium and depending on the ratio of relaxation time to characteristic heat dissipation time. Article was presented by Academician V.I. Goldanskiy on 30 December 1988. Figures 2; references 6

UDC 538.945

Thermal Conductivity of High-Temperature Superconductors in Normal State

907L0076A Kharkov FIZIKA NIZKIKH
TEMPERATUR in Russian Vol 15 No 10, Oct 89
pp 1025-1031

[Article by A. Jezowski, J. Klamut, and J. Trojnar, Institute of Low Temperatures and Structural Analysis, Polish Academy of Sciences, Wroclaw/ POLAND]

[Abstract] Available experimental data on high-temperature superconductors are analyzed concerning the thermal conductivity of these materials in the normal state above the superconducting transition temperatures. The materials included here are $\text{YBa}_2\text{Cu}_3\text{O}_{7-d}$ ($d = 0.19, 0.46, 0.90$), (Sm, Eu, Gd, Ho, Er)-Ba-Cu-O, and Tl-Ba-Ca-Cu-O metal oxides, their thermal conductivity having been measured over the 5-320 K temperature range. The main conclusions are that only the maximum value of the thermal conductivity depends on the oxygen content in a metal-like and therefore superconducting material, it increases with increasing oxygen content, while the trend of its temperature dependence above the critical temperature does not. The temperature at which the slope of the conductivity-temperature curve changes abruptly does, however, shift depending on the oxygen content just as the superconducting transition temperature does. Accordingly, the thermal conductivity of materials with a low oxygen content and therefore non-superconducting ones has no maximum and there occurs no abrupt change of slope along its temperature characteristic. More conclusions are drawn by reference to the

Wiedemann-Franz law, calculations revealing that the electronic component of thermal conductivity is higher when the oxygen content is higher and reaches 20% of the total thermal conductivity for materials with the highest oxygen content. Overall estimates are made, considering that the phononic component is dominant in the thermal conductivity of those high- T_c superconductor materials. Measurements have revealed a weak anomaly of the thermal conductivity along its otherwise linear temperature dependence, this anomaly being analogous to that of the electrical resistivity along its otherwise linear temperature dependence and occurring at about 250 K for the Y-Ba-Cu-O materials. This anomaly is hypothetically attributed to ordering of the oxygen vacancies. Measurements covering both orthorhombic and tetragonal forms of Y-Ba-Cu-O and other 1:2:3 materials have revealed a hysteresis of their thermal conductivity within and somewhat above the superconducting transition. It is evidently attributable to structural phase transitions, which occur within this temperature range, inasmuch as no such hysteresis has been revealed by a study of La_2CuO_4 materials with excess oxygen ($\text{La}_{1.65}\text{CuO}_{4+e}$ and nonsuperconducting $\text{La}_{2.1}\text{CuO}_{4+e}$). This study revealed a similar anomaly of their thermal conductivity within the 200-290 K range, however, which must evidently be attributed to structural phase transition. Figures 8; references 23

UDC 538.945

Superconductivity of Oxide Film Electrolytically Deposited on Surface of $\text{Bi}_{1-x}\text{Sb}_x$ Single Crystal

907L0076B Kharkov FIZIKA NIZKIKH
TEMPERATUR in Russian Vol 15 No 10, Oct 89
pp 1099-1101

[Article by V.N. Alfeyev, B.A. Aminov, N.B. Brandt, S.Ya. Vasina, B.B. Damaskin, M. Zigel, V.P. Kuznetsov, O.A. Petriy, Ya.G. Ponomarev, M.V. Sudakova, and Ye.G. Frank, Moscow State University imeni M.V. Lomonosov]

[Abstract] An experimental study was made of thin oxide films electrolytically deposited on the surface of $\text{Bi}_{1-x}\text{Sb}_x$ single crystals (x from 0.1 to 0.3) at room temperature, the electrolyte consisting of acetonitrile as solvent with salicylic acid as conductive additive and containing copper ions. The current-voltage characteristics of point junctions produced by mechanical pressure on oxidized surfaces were measured at temperatures ranging from 1.7 K to above 20 K. They were in most cases found to be characteristics of Josephson junctions, with a critical current in the milliampere range at 4.2 K, with Mersero constant-period oscillations of the differential electrical conductance dI/dV near zero voltage in a magnetic field,

and with Shapiro plateaus in a microwave field. The critical temperature of superconducting transition corresponding to maximum differential electrical conductance near zero voltage was found to be within 6-8 K in most cases and 20 K or higher in some cases. Figures 3, references 4

UDC 537.312

Effect of Hydrogen on $\text{YBa}_2\text{Cu}_3\text{O}_y$ Ceramic With $y = 6.91$ and 6.54

907L0063A Leningrad FIZIKA TVERDOGO TELA
in Russian Vol 31 No 12, Dec 89 pp 54-61

[Article by V.V. Sinitsyn, I.O. Bashkin, Ye.G. Ponyatovskiy, V.M. Prokopenko, R.A. Dilanyan, V.Sh. Shekhtman, M.A. Nevedomskaya, I.N. Kremenskaya, N.S. Sidorov, R.K. Nikolayev, and Zh.D. Sokolovskaya, Institute of Solid-State Physics, USSR Academy of Sciences, Chernogolovka (Moscow Oblast)]

[Abstract] An experimental study of $\text{YBa}_2\text{Cu}_3\text{O}_y$ ceramics with $y = 6.91, 6.54, 6.05$ was made, for the purpose of determining the dependence of their structural and superconductivity characteristics on the hydrogen concentration in them. Specimens of these ceramics were hydrogenated at temperatures of 363-373 K so as to ensure minimum chemical interaction, whereupon the mean copper oxidation level was determined on the basis of chemical analysis by iodometric titration and the oxygen content was determined on the basis of thermogravimetric analysis. Superconducting transition, monitored by the induction method, was indicated by the anomaly in the temperature dependence of the magnetic susceptibility with two temperatures identifying the transition range: its beginning at T_{co} and its midpoint at T_{cm} . Structural examination yielding the lattice parameters and the phase composition was done in a DRON-3 x-ray diffractometer with a $\text{CuK}\alpha$ -radiation source. The results indicate no decrease of the total oxygen content upon hydrogenation up to an $x = 1.5$ concentration in the $\text{YBa}_2\text{Cu}_3\text{O}_{6.91, 6.54} \text{H}_x$ ceramic, nor significant changes of T_{co} temperature. The mean copper oxidation level z was found to decrease almost linearly with increasing hydrogen concentration x above $x = 0.15$, where this relation extrapolates to $z(x) = 2.25 - 0.35x$ for $y = 6.91$ and to $z(x) = 2.02 - 0.35x$ for $y = 6.54$. The observed decrease of the volume of the superconducting phase is probably caused by interaction of hydrogen and Cu-ions within the solid solution rather than by of an amorphous nonsuperconducting phase. Figures 5; references 17

UDC 537.312.62

Transformation of Acoustic Wave at Piezocrystal-Superconductor Boundary

907L0063B Leningrad FIZIKA TVERDOGO TELA
in Russian Vol 31 No 12, Dec 89 pp 114-119

[Article by V.I. Alshits and V.N. Lyubimov, Institute of Crystallography imeni A.V. Shubnikov, USSR Academy of Sciences, Moscow]

[Abstract] Reflection of an acoustic wave in a crystal with piezoelectric and piezomagnetic properties at the boundary of such a crystal with a superconductor and specifically a high- T_c superconductor is analyzed, it being known that the piezomagnetic part "senses" the contiguous superconductor and the piezoelectric part "senses" the contiguous normal metal. For simplicity is considered where only both phase and amplitude of an elastic displacement wave but not its polarization change upon reflection. The crystal is assumed to be transversely isotropic and its boundary with the superconductor to be a plane parallel to its principal axis of symmetry, the plane of incidence on that boundary being perpendicular to it. Relations which yield the reflection coefficient and indicate the transformation of an incident acoustic shear wave are derived for a boundary between freely sliding bodies, with the superconductor material either in the dielectric state or in the normal metallic state, for a mechanically rigid contact between the two bodies, and for a superconductor film on a piezocrystalline substrate. A relation is obtained for calculating the volume fraction of the superconducting phase and the expression for the loss tangent is extended so as to also include absorption. The results of this analysis indicate that the phase composition of a superconducting material can be monitored with the aid of an electric or magnetic field and acoustic waves. References 9

UDC 539.4.096:536.48

Kinetics of Polymer Breakdown at Moderate and Low Temperatures

907L0063C Leningrad FIZIKA TVERDOGO TELA
in Russian Vol 31 No 12, Dec 89 pp 120-125

[Article by A.I. Slutsker, T.M. Veliyev, I.K. Aliyeva, and S.A. Abasov, Institute of Engineering Physics imeni A.F. Ioffe, USSR Academy of Sciences]

[Abstract] An experimental study of three nonoriented hybrid amorphous-crystalline carbon-chain polymers (polyethylene, polyethylene terephthalate, polytetrafluoroethylene) was made in which the temperature-stress dependence of their durability was determined by direct measurements at 90-250 K temperatures and 75-330 MPa pressures, these polymers having been selected on

account of their supermolecular structure with rather few "intermediate" chain molecules and the correspondingly specific mode of rupture of interatomic bonds under load. The durability life (time τ , s) and temperature (T, K) data are presented in $\log \tau, T$ semilog coordinates and in $\log \tau, 1/T$ "Arrhenius" coordinates. They indicate athermal breakdown kinetics at low temperatures and temperature-dependent breakdown kinetics in the range of moderate temperatures, the transition from one mechanism occurring at a lower temperature under a higher pressure. Other data include stress-strain relation at low temperatures and the temperature dependence of tensile strain at rupture, which characterizes the ductility of these materials. A statistical analysis based on at least 12 samples of each material has yielded a nearly normal durability distribution at all temperatures. Figures 4; references 14

UDC 54-11

New Phases in Tl-Ca-Ba-Cu-O and Bi-Ca-Sr-Cu-O Systems

907L0108A Moscow DOKLADY AKADEMII NAUK
SSSR in Russian Vol 310 No 2, 20 Jan 90 pp 337-339

[Article by N.Ye. Alekseyevskiy, corresponding member, USSR Academy of Sciences, G.M. Kuzmicheva, Ye.P. Khlybov, T.N. Tarasova, and V.I. Nizhankovskiy, Institute of Problems in Physics imeni S.I. Vavilov, USSR Academy of Sciences, Moscow]

[Abstract] An experimental study of a Ca-Ba-Cu-O compound with Tl and a Ca-Sr-Cu-O compound with Bi was

made involving preparation of specimens and subsequent measurement of their crystallographic parameters and specific heat as well as the temperature dependence of their electrical resistivity and magnetic susceptibility. A mixture of CaO, BaO, CuO and metallic Tl corresponding to $Tl_2Ca_2Ba_2Cu_3O_8$ was sintered in a furnace at 850°C for 2-5 min and quenched in air, whereupon the product was grated into powder, the powder was pressed into compacts, and the latter were annealed at 850°C for 1-8 h. Mixtures of CaO, SrO, CuO and metallic Bi or Bi_2O_3 were treated analogously. The measurements revealed, in addition to the already known phases I, III, IV, V in the Bi-ceramic and phases I, II, IV, V in the Tl-ceramic, also a new phase VI with a lattice parameter $c = 3.95$ nm in both ceramics. A characteristic feature of the Tl-ceramic containing phase VI was a nonlinear temperature dependence of its electrical resistivity above the critical temperature. Duplicating the known technology of adding Tl_2O_3 rather than metallic Tl and, after completion of the synthesis at 900°C, slow in the furnace did not produce a superconductor Tl-ceramic with a critical temperature $T_c = 162$ K but instead yielded a semiconductor material with no superconducting transition at all. Synthesis with metallic Tl at 900°C for 5 min, annealing at 600°C for 1 h, and cooling at a rate of 3°C/min yielded a material with a critical temperature $T_c = 110$ K, this material consisting of phase V as principal component (approximately 80%) and the new phase VI. The temperature dependence of its electrical resistivity was linear above 160 K, indicating a metallic behavior, and nonlinear below 160 K. The highest critical temperature attained in this study by optimization of the technology was $T_c = 122$ K. The authors thank Ye.G. Nikolayev for discussing the results, M.G. Mikheyev and Yu.A. Deniskin for assisting in the measurements. Figures 2; tables 1; references 9

Stochastic Model of Quantum Mechanics

907L0115A Moscow *TEORETICHESKAYA I
MATEMATICHESKAYA FIZIKA in Russian Vol 82*
No 2, Feb 90 pp 208-215

[Article by V.Yu. Podlipchuk, Moscow Institute of
Radio Engineering, USSR Academy of Sciences]

[Abstract] The problem of correlating quantum mechanics with the theory of random processes is resolved by construction of a stochastic model on the basis of the plain theory of probability in terms of distribution functions. A correspondence is accordingly established between the Schroedinger wave equation and a real nonnegative probability density function which describes the dynamics of a Markov process in the complex phase space and yields all quantum mean values. A complex and thus quasi-probability function is introduced and its properties are demonstrated, as a preliminary step toward resolution of the problem, the two-parametric quasi-probability function $w(x,p)$ matching the two one-parameter distribution functions $w(x)$ and $w(p)$ when a state is described by the density matrix $\rho(x,x')$. The partial differential equation for this quasi-probability function is derived from the quantum extension of the Liouville equation for the density matrix by expanding the potential $U(x')$ into a Taylor series at point x and performing a Fourier transformation with respect to x' on both sides of that equation. Complex random processes are then described by ordinary stochastic differential equations according to the same rules that apply to the Fokker-Planck equation with a positive diffusion coefficient, imaginary diffusion coefficients in this case generating complex stochastic differential equations. The special case of quasi-classical

stochastic differential equations is considered next, whereupon stationarity and invertibility of all these stochastic differential equations are briefly touched upon. The author thanks A.A. Valuyev, A.S. Kaklyugin, and G.E. Norman for the discussion

**New Mechanism of Particle Acceleration and
Rotation Number Increase**

907L0115B Moscow *TEORETICHESKAYA I
MATEMATICHESKAYA FIZIKA in Russian Vol 82*
No 2, Feb 90 pp 257-267

[Article by L.D. Pustynnikov, All-Union Scientific
Research Institute of Electric Power Engineering]

[Abstract] Two mathematical models are constructed to describe real physical processes in which the energy of particles, particularly of charged ones, increases infinitely within an arbitrarily small space. They are based on the relativistic analog of the Fermi-Ulam model and apply to a particle which like a ball moving in the vertical direction between two infinitely heavy horizontal walls periodically in time, upon elastically bouncing off the lower wall, continues oscillating periodically in time and vertically as if it had elastically collided with an infinitely heavy third wall parallel to the other two. The first model is constructed for the special case of a stationary upper wall and a vertically moving lower wall, its validity being based on four theorems. The second model is constructed for the other special case of three walls, this model being validated by three additional theorems. According to these models, the energy of a particle increases infinitely with the lower bound of the energy increment corresponding to an asymptotically small distance between the walls. Figures 2; references 5

UDC 519.63

Numerical-Asymptotic Method of Multicomponent Averaging of Equations With Contrasting Coefficients

907L0088A Moscow ZHURNAL VYCHISLITELNOY
MATEMATIKI I MATEMATICHESKOY FIZIKI
in Russian Vol 30 No 2, Feb 90 pp 243-253

[Article by G.P. Panasenko, Moscow]

[Abstract] A new numerical-asymptotic method of multicomponent averaging is proposed for solution of partial differential equations with contrasting coefficients which describe processes in periodic multicomponent and thus strongly nonhomogeneous media, such equations generally containing two parameters: ratio ε of structural period to characteristic dimension is a measure of fineness and ratio ω of the values of a constant which characterizes a physical property of the material components is a measure of their contrast. The coefficients in such equations are generally also fast oscillating functions of space variables and the asymptotic behavior of their solutions as $\varepsilon \rightarrow 0$ and $\omega \rightarrow \infty$ depends on the relation between these two parameters. The method of multicomponent averaging is an adaptation of the small-parameter method to nonlinear equations of this kind with $\varepsilon^2\omega \rightarrow \infty$ or $\varepsilon^2 = \text{const}$ as well as to linear equations of this kind with $\varepsilon^2\omega \rightarrow 0$. Nonlinear equations of this class are found in problems of diffusion and heat conduction, with homogeneous initial conditions and with boundary conditions of the second kind. References 8

UDC 519.62

Localized Solutions to Second-Order Nonlinear Differential Equation

907L0088B Moscow ZHURNAL VYCHISLITELNOY
MATEMATIKI I MATEM. FIZIKI in Russian Vol 30
No 2, Feb 90 pp 319-320

[Article by B.V. Gisin, Moscow]

[Abstract] Analyzing the propagation of a TM-mode wave through a nonlinear medium leads, under certain simplifying assumptions, to the equation $(R' + R/r)' = R - R^2 + \alpha(R' + R/r)^2$ and requires finding solutions to it which are continuous solutions in the region of nonnegative r but bounded as is also the derivative at r approaching infinity. This equation has two kind of such solutions corresponding respectively to two different series expansions of $R(r)$ at r approaching infinity, one representing TM_{IN} -modes in a plain linear waveguide and one kind being "free" solutions. The eigenvalues R_1 , which depend on α as well as on R_0 , are obtained from the condition that all $R(r)$ terms those series expansions tend to become a MacDonald functions as r approaches infinity. One condition for validity

of this equation is that α be small and physically important are only solutions for positive α , TM_{IN} solutions for negative α fast becoming indeterminate as α approaches infinity so that asymptotic solutions must be obtained at increasingly larger r_0 . References 3

Stability Criterion for Solitons

907L0105A Moscow TEORETICHESKAYA I
MATEMATICHESKAYA FIZIKA in Russian Vol 82
No 1, Jan 90 pp 28-33

[Article by A.B. Givental, Institute of Chemical Physics,
USSR Academy of Sciences]

[Abstract] The equation $\ddot{u} = (-u_{xxx} + f(u_x))_x$ describing longitudinal vibrations of an infinitely long beam is analyzed for stability of its soliton solutions in the space of functions u of variable x , this equation also representing a system with kinetic energy T and potential energy V in the Lagrangian formulation. In the expression for V (Integral of $(1/2)u_{xx}^2 dx + f(u_x) dx$ from $-\infty$ to $+\infty$) x denotes displacement, $f(u_x) dx$ denotes the energy density of the strain field, and u_{xx}^2 adds dispersion to the equation of small vibrations. A spherical ball of unity mass rolling along the v -axis in a potential field $g(v) = (1/2)c^2(v - \varepsilon)^2 + f(\varepsilon)v - f(v)$ is considered, point $v = \varepsilon$ being its equilibrium position. When $c^2 < f''(\varepsilon)$, then this equilibrium is unstable so that an aperiodic motion $v(y) \rightarrow \varepsilon$ at y approaching $-\infty$ or $+\infty$ is possible and that equation thus has a solution which describes a soliton moving at a velocity $+c$ or $-c$ in a strain field. Following linearization of the corresponding Hamiltonian in the phase space, the equilibrium position of a typical linear Hamiltonian system with stationary points along a straight line being unstable, the stability problem for a traveling wave in such a system is solved in the vicinity of any given equilibrium position. From the quadratic Hamiltonian of the h^{ct} flux replacing the g^t flux and linearized at a stationary point is derived the stability criterion for such a soliton, considering that this flux corresponding to a soliton has the signature $(-, 0, 0, +, +, \dots)$ and that there exists a pair of invariant planes in which its Hamiltonian is equivalent to $(1/2)p^2$ and $-$ or $+(1/2)p^2$ respectively. The linear Hamiltonian system, meanwhile, has an invariant plane generated by the eigenvector $(p, q) = (0, 1)$ and the conjugate vector $(p, q) = (1, 0)$, its constraints on these planes having the signature $(+, 0)$. Taking into account the additional invariant subspace of bounded functions (p, q) with zero mean values and invariant planes of the system in this space, Sturm's theorem is extended to a quadratic functional S with higher-order derivatives and smooth positive coefficients, to prove that the Lagrangian of a soliton has the signature $(-, 0, 0, +, +, \dots)$. The stability criterion is demonstrated on a soliton in a system with a cubic potential $f = (1/2)c_0^2 u^2 + (1/3)u^3$. The author thanks A.V. Dobrynin, L.I. Manevich, and V.V. Smirnov for interest and many discussions. References 7

Comment on Quantization of Hydrogen Atom by Continuous Integral Method

907L0105B Moscow *TEORETICHESKAYA I MATEMATICHESKAYA FIZIKA in Russian* Vol 82 No 1, Jan 90 pp 47-54

[Article by S.N. Storchak, Institute of High-Energy Physics]

[Abstract] The continuous integration method developed earlier for random processes is applied to quantization of a hydrogen atom, two independent transformations being required for this: reparametrization of the integration paths and Kustaanheimo-Stiefel transformation. The continuous integral representing Green's function in the phase space for a hydrogen atom is an integral with respect to the measure generated by the corresponding random process so that reparametrization through time is characterized by a nonzero Jacobian and will yield a Wiener integral rather than a Feynman continuous one. The subsequent K-S transformation is performed in spherical coordinates, considering not only that each probability density is representable as an integral of a measure generated by a random process but also that all measures must be generated by random processes of the same kind. Insofar as random processes in a hydrogen atom are described by stochastic differential equations of the Stratonovich kind, Laplace-Beltrami operators have been selected as such generators so that the quantization rule for a classical Hamiltonian which includes terms linear with respect to momenta is retained as long as the term without derivative is treated as a potential. Another transformation, a point transformation from variable $(r, \theta, \phi, \alpha)$ to variables (u_1, u_2, u_3, u_4) is still needed for relating Green's function for a hydrogen atom to a four-dimensional harmonic oscillator. The author thanks B.A. Arbuzov and A.I. Oksak for discussion and helpful comments. References 12

New Method of Calculating Phase of Radial Wave Function for Scattering by Spherically Symmetric Potential

907L0013A Moscow *ZHURNAL EKSPERIMENTALNOY I TEORETICHESKOY FIZIKI in Russian* Vol 96 No 5, Nov 89 pp 1587-1597

[Article by T.M. Bandman and S.G. Rautian, Institute of Automation and Electrometry, Siberian Department, USSR Academy of Sciences]

[Abstract] A new method of solving the radial wave equation with one reversal point is proposed, namely by representing the solution as the sum of two functions such that an exact first-order differential equation is obtained for the phase shift everywhere and without singularities at the reversal point. In this way it becomes unnecessary to analyze the equation in the nonclassical

region and the boundary conditions can be stipulated directly at the inversion point, nor is it necessary to analyze the solution in the vicinity of singularities. Initial conditions are stipulated after the wave function has been expanded at the inversion point into an asymptotic series in a dimensionless small parameter. The method is applied to scattering by a centrisymmetric potential, this problem being reduced by standard procedure to a one-dimensional equation for the radial multiplier of the wave function. This problem has been solved numerically for a $k^2 = l(l+1)(1-z^2)$ potential and for a Lennard-Jones potential. The solution in the third approximation is compared with the solution in the first approximation according to the Wentzel-Kramer-Brillouin method and found to be more accurate, an advantage of the new method being that calculation in any order approximation does not require the solution in the preceding order approximation. Figures 5; tables 1; references 10

Coherent Effects in Generation of Ultrashort Light Pulses by Semiconductor Injection Laser

907L0013B Moscow *ZHURNAL EKSPERIMENTALNOY I TEORETICHESKOY FIZIKI in Russian* Vol 96 No 5, Nov 89 pp 1629-1637

[Article by E.M. Belenov and P.P. Vasilyev, Institute of Physics imeni P.N. Lebedev, USSR Academy of Sciences]

[Abstract] Pulsed emission of coherent light by a two-level semiconductor as active medium of an injection laser with a new kind of Q-switching is analyzed for the case of pulse duration longer than the zero-field polarization relaxation time at the second level $T_2(0)$, this relaxation time becoming longer in the presence of an electric field and more so as the field intensity increases so that in a strong field $T_2(E)$ may be longer than the pulse duration. Pulses shorter than 5 ps with a power flux density in the GW/cm^2 range are considered, a power density sufficient for stimulated Raman scattering of active modes also during coherent light conversion with suppressed scattering-phase relaxation. The theoretical analysis is based on a system of Maxwell-Bloch equations which describes the dynamics of coherent radiation emission for an injection laser with a very high excess above threshold inversion. An experiment was performed with an AlGaAs/GaAs heterojunction injection laser and that new method of Q-switching, to ensure formation of high-power ultrashort pulses. It revealed the conditions for and the characteristics of stimulated Raman scattering during generation of picosecond pulses. On the basis of these data and theoretical considerations, is predicted the feasibility of generating femtosecond pulses in such an injection laser by means of stimulated Raman scattering, which suppresses field oscillations. Figures 4; references 14

UDC 517.9:519.3

Extremal Solutions to Some Systems of Differential-Operator Equations

907L0059A Kiev UKRAINSKIY MATEMATICHESKIY ZHURNAL in Russian Vol 41 No 11, Nov 89 pp 1494-1501

[Article by V.S. Melnik, Institute of Cybernetics, UkSSR Academy of Sciences, Kiev]

[Abstract] Extremal properties of solutions to systems of differential-operator equations $y' + A(z, y) = f$ with $y(t=0) = y_0$, $z = G(u, z, y) + g$, and $F(u, z, y) \geq 0$ (u member of set U in Banach space U , z member of set M in Banach space Z , y member of set K in Banach space X) appearing in control theory are analyzed, following a concretization of the control objects and a definition of two relevant multiple-valued mappings as well as a definition of an L_1 -extremal solution to such a system of equations. A proposition is stated which leads to two relevant corollaries, whereupon four theorems are proved. The first theorem is proved with the aid of three lemmas, the first one leading to two corollaries and the other two leading to a third corollary. The second theorem leads to two more corollaries and the other two theorems are extensions of the first one. References 10

UDC 517.9

Asymptotic Behavior of Solutions to One Class of Differential-Functional Equations

907L0059B Kiev UKRAINSKIY MATEMATICHESKIY ZHURNAL in Russian Vol 41 No 11, Nov 89 pp 1526-1532

[Article by Ye.Yu. Romanenko, Institute of Mathematics, UkSSR Academy of Sciences, Kiev]

[Abstract] The asymptotic behavior of $C^1(0, T)R$ solutions to the equation $dx/dt(at) + t^\gamma b(t)dx/dt(t) + c(t)x(at) + d(t)x(t) = 0$ ($0 < \gamma < 1$ and $a > 1$) within the neighborhood its critical point $t = 0$ is analyzed, assuming that functions $b, c, d: R^+ \rightarrow R$ are continuous and $b(0) = b$ is not equal to zero. A four-part theorem is proved with the aid of three lemmas pertaining to existence of a solution, to the majorant, and to an auxiliary estimate respectively, whereupon the general solution to that equation within the neighborhood of $t = 0$ is obtained by the method of successive approximations. The theorem extends to quasi-linear equations $dx/dt(at) + t^\gamma b(t)dx/dt(t) = f(t, x(t), x(at))$ ($0 < \gamma < 1$ and $a > 1$) with Lipschitz right-hand sides f , $f(t, 0, 0) = 0$. References 3

UDC 517.9+512.7

Commutating Differential Operators of Rank 3 and Nonlinear Equations

907L0049A Moscow IZVESTIYA AKADEMII NAUK SSSR: SERIYA MATEMATICHESKAYA in Russian Vol 53 No 6, Nov-Dec 89 pp 1291-1314

[Article by O.I. Mokhov]

[Abstract] Deformation in y and t of general solutions to the Kadomtsev-Petviashvili commutativity equation for $l = 3$ and $g = 1$ is analyzed and a closed system of equations readily integrable with respect to t is obtained for deformation of Tyurin parameters. For a system of equations for the coefficients of two scalar ordinary differential operators are L_1, L_2 are, on the basis of two known theorems aided by two lemmas, are established three general analytical properties of a pair of commuting differential operators which properties together with two sets of arbitrary constants γ_i, α_{ij} and generally $l-2$ arbitrary functions $w(x)$ determine the corresponding vector-function as well as the commuting pair L_1, L_2 of l -th rank in common position. Then, on the basis of a new theorem proved with the aid of two lemmas, the system of Krichever-Novikov equations is integrated for rank 3 and first kind. Explicit expressions for commuting operators of rank 3 and first kind are derived on the basis of a second new theorem. The algebraic properties of functional parameters which govern commuting operators with rational coefficients are established on the basis of a third new theorem and a corollary proved with the aid of four lemmas. The necessary and sufficient conditions for rationality of these coefficients are established on the basis of two new theorems proved with the aid of one lemma each. Finally, solutions to the Kadomtsev-Petviashvili equation are obtained by deformation of a pair of commuting differential operators and then the equation of deformation for such operators of rank 3 and first kind is solved on the basis of a proposition and a lemma leading to a sixth new theorem. References 40

UDC 519.21

Periodic Solutions to Differential Equations of Evolution Perturbed by Random Processes

907L0055A Kiev UKRAINSKIY MATEMATICHESKIY ZHURNAL in Russian Vol 41 No 12, Dec 89 pp 1642-1648

[Article by A.Ya. Dorogovtsev, Kiev University]

[Abstract] Two differential equations of evolution perturbed by any periodic random process are considered in a complex separable Banach space, one equation with a bounded operator and one equation with a sectorial unbounded one generating an analytic subgroup of bounded ones in that Banach space. For both equations are proved two theorems which establish the conditions for existence and uniqueness of a periodic solution

certain to have strongly continuously differentiable trajectories, this both necessary and sufficient condition being that the operator spectrum does not intersect the imaginary axis. References 4

UDC 517.9

Reducibility of System of Linear Differential Equations With Quasi- Periodic Coefficients

907L0055B Kiev UKRAINSKIY MATEMATICHESKIY ZHURNAL in Russian Vol 41, No 12, Dec 89
pp 1669-1680

[Article by A.M. Samoilenko, Institute of Mathematics, UkSSR Academy of Sciences]

[Abstract] A reducibility theorem analogous to the measure theorem for a system of linear differential equations with quasi-periodic coefficients is proved on the basis of two theorems pertaining to such equations with an n -dimensional matrix $P(\varphi, \varepsilon)$ 2π -periodic in $\varphi = (\varphi_1, \dots, \varphi_m)$ as well as analytic in (φ, ε) and a fixed vector $\omega = (\omega_1, \dots, \omega_m)$ of frequencies of matrix $P(\omega t, \varepsilon)$, considering an $N(\alpha, \beta, \gamma)$ - $n=(d+2p)$ -parametric family of $N(\alpha, \beta, \gamma)$ matrices. An outline of the proof and an analysis of the dependence of the solution to such an equation on parameter ε reveal a "loss of smoothness" with respect to this parameter, owing to generally existing complex-conjugate eigenvalues of the N -matrix. There follows a theorem for the special case of $d = n$, which corresponds to an N -matrix with only real eigenvalues so that the solution remains smooth with respect to ε , and then a theorem for $n = 2$. References 5

UDC 517.925.51

Criteria for Asymptotic Stability of Systems of Differential Equations With Periodic Coefficients

907L0061A Moscow DIFFERENTIALNYE URAVNENIYA in Russian Vol 25 No 12, Dec 89
pp 2059-2066

[Article by N.Ye. Barabanov, Leningrad Institute of Electrical Engineering imeni V.I. Ulyanov (Lenin)]

[Abstract] The system of differential equations $dx(t)/dt = (A + b(t)c^*)x(t)$ (A - constant $n \times n$ Hurwitz matrix, $x(\cdot)$ - absolutely continuous n -dimensional vector-function,

b, c - constant n -dimensional vectors, $a(\cdot)$ - bounded scalar T_0 -periodic function, all quantities real) with a transfer function $W(s) = c^*(A - sI)^{-1}b$ is analyzed for asymptotic stability. Three theorems are proved which establish criteria for asymptotic stability of this system. The general criterion, stated in the form of a necessary and sufficient condition, is existence of a certain kind of solutions for all y 's in the R^n -space and all z 's in C^+ -space. The more simply stated other two criteria are more restrictive, constraining respectively the sum of the series $\sum |W(z + ij\omega)| |a_{k-j}|$ over all j 's from $-\infty$ to $+\infty$ ($k = 0$, positive and negative integers) to be not larger than some q in set $(0, 1)$ for all z 's in the C^+ -space and the sum of the series $\sum |W(z + ik\omega)| |a_{k-m}| + |W(z) a_{-m}| / C$ with some positive numbers C over all positive and negative k 's ($m =$ positive and negative integers) to be not larger than some q in set $(0, 1)$ for all z 's in the T -space. A system of two first-order differential equations with mutually orthogonal harmonic parametric perturbations is considered next and three theorems are proved which establish conditions for its asymptotic stability. References 2

UDC 517.928

Existence of Average Differential Inclusion

907L0061B Moscow DIFFERENTIALNYE URAVNENIYA in Russian Vol 25 No 12, Dec 89
pp 2118-2127

[Article by O.P. Filatov, Moscow Institute of Technology, Tolyatti branch]

[Abstract] A system of differential inclusions with fast and slow variables dx/dt in set $\mu F(t, x, y, \mu)$ and dy/dt in set $G(t, x, y, \mu)$, $x(t_0) = x_0$ and $y(t_0) = y_0$, is analyzed for existence and uniqueness of an average inclusion. The problem of mutual ε -approximation is formulated for this system, with several assumptions made with regard to multiple-valued mapping of F in region D into $K_v(R^m)$. Two theorems are then proved, the first one with the aid of 11 lemmas establishing the existence of transform F_0 in region P ($D = D_0 X [0, \mu^0]$, $D_0 = R^+ \times P \times Q$, P in the R^m -space, Q in the R^n -space, $R^+ = [0, +\infty)$) under those and several other assumptions and the second one pertaining to equality of two differential inclusions with continuous transforms when they mutually ε -approximate that system of differential inclusions with respect to slow variables. The author thanks M.M. Khapayev for discussion. References 7

UDC 512.81

Ergodic Expansion of Fluxes on Homogeneous Spaces of Finite Volume

907L0068A Moscow *MATEMATICHESKIY SBORNIK*
in Russian Vol 180 No 12, Dec 89 pp 1614-1633

[Article by A.N. Starkov, All-Union Institute of Electrical Engineering imeni V.I. Lenin, Istra branch]

[Abstract] A complete proof is given regarding ergodic expansion of fluxes on homogeneous spaces of finite volume, a G -induced or homogeneous flux $(G/D, e^{tx})$ which acts according to the rule $gD \rightarrow e^{tx}gD$. Three

theorems pertaining to such a flux and a review of relevant concepts in the theory of algebraic groups are followed by three theorems and four propositions pertaining to homogeneous spaces of finite volumes, proved and illustrated with examples. Ergodic expansion in general and some of its forms are described with the aid of five lemmas and seven corollaries leading to a statement which completes the proof of the three introductory theorems. There follows a discussion of still unresolved problems which pertain to the mixing criterion $G = \text{over } I_x D$ for a $(G/D, e^{tx})$ flux. In conclusion the author disproves two corollaries stated by M. Ragunatan (?) pertaining to discrete subgroups of a Lie group. References 20.

22161

21

NTIS

ATTN: PROCESS 103
5285 PORT ROYAL RD
SPRINGFIELD, VA

22161

This is a U.S. Government publication. Its contents in no way represent the policies, views, or attitudes of the U.S. Government. Users of this publication may cite FBIS or JPRS provided they do so in a manner clearly identifying them as the secondary source.

Foreign Broadcast Information Service (FBIS) and Joint Publications Research Service (JPRS) publications contain political, military, economic, environmental, and sociological news, commentary, and other information, as well as scientific and technical data and reports. All information has been obtained from foreign radio and television broadcasts, news agency transmissions, newspapers, books, and periodicals. Items generally are processed from the first or best available sources. It should not be inferred that they have been disseminated only in the medium, in the language, or to the area indicated. Items from foreign language sources are translated; those from English-language sources are transcribed. Except for excluding certain diacritics, FBIS renders personal and place-names in accordance with the romanization systems approved for U.S. Government publications by the U.S. Board of Geographic Names.

Headlines, editorial reports, and material enclosed in brackets [] are supplied by FBIS/JPRS. Processing indicators such as [Text] or [Excerpts] in the first line of each item indicate how the information was processed from the original. Unfamiliar names rendered phonetically are enclosed in parentheses. Words or names preceded by a question mark and enclosed in parentheses were not clear from the original source but have been supplied as appropriate to the context. Other unattributed parenthetical notes within the body of an item originate with the source. Times within items are as given by the source. Passages in boldface or italics are as published.

SUBSCRIPTION/PROCUREMENT INFORMATION

The FBIS DAILY REPORT contains current news and information and is published Monday through Friday in eight volumes: China, East Europe, Soviet Union, East Asia, Near East & South Asia, Sub-Saharan Africa, Latin America, and West Europe. Supplements to the DAILY REPORTs may also be available periodically and will be distributed to regular DAILY REPORT subscribers. JPRS publications, which include approximately 50 regional, worldwide, and topical reports, generally contain less time-sensitive information and are published periodically.

Current DAILY REPORTs and JPRS publications are listed in *Government Reports Announcements* issued semimonthly by the National Technical Information Service (NTIS), 5285 Port Royal Road, Springfield, Virginia 22161 and the *Monthly Catalog of U.S. Government Publications* issued by the Superintendent of Documents, U.S. Government Printing Office, Washington, D.C. 20402.

The public may subscribe to either hardcover or microfiche versions of the DAILY REPORTs and JPRS publications through NTIS at the above address or by calling (703) 487-4630. Subscription rates will be

provided by NTIS upon request. Subscriptions are available outside the United States from NTIS or appointed foreign dealers. New subscribers should expect a 30-day delay in receipt of the first issue.

U.S. Government offices may obtain subscriptions to the DAILY REPORTs or JPRS publications (hardcover or microfiche) at no charge through their sponsoring organizations. For additional information or assistance, call FBIS, (202) 338-6735, or write to P.O. Box 2604, Washington, D.C. 20013. Department of Defense consumers are required to submit requests through appropriate command validation channels to DIA, RTS-2C, Washington, D.C. 20301. (Telephone: (202) 373-3771, Autovon: 243-3771.)

Back issues or single copies of the DAILY REPORTs and JPRS publications are not available. Both the DAILY REPORTs and the JPRS publications are on file for public reference at the Library of Congress and at many Federal Depository Libraries. Reference copies may also be seen at many public and university libraries throughout the United States.